NUMERICAL SOLUTION TO MATHEMATICAL MODELS OF INFECTIOUS DISEASES

by

Priscilla Oghaleoghene OBADONI (Miss)

PSC2105450

DEPARTMENT OF MATHEMATICS

FACULTY OF PHYSICAL SCIENCE

UNIVERSITY OF BENIN

BENIN CITY

OCTOBER,2025

CERTIFICATION

This is to certify that this project titled, "**APPROXIMATE SOLUTION TO MATHEMATICAL MODEL OF INFECTIOUS DISEASES USING EXPLICIT STAGE TWO RUNGE-KUTTA PROCESSES"** was done by **Priscilla Oghaleoghene OBADONI** with matriculation number **PSC2105450** in partial fulfillment for the award of the degree of Bachelor of Science in Industrial Mathematics, Department of Mathematics, Physical Sciences, University of Benin, Benin City.

_____ _____

PROF. K.O MUKA Date

(Project Supervisor)

_____ _____

PROF. D. OKUONGHAE Date

(HEAD OF DEPARTMENT)

DECLARATION

I, Priscilla Oghaleoghene OBADONI, declare that this project work titled "**APPROXIMATE SOLUTION TO MATHEMATICAL MODEL OF INFECTIOUS DISEASES USING EXPLICIT STAGE TWO RUNGE-KUTTA PROCESSES"** submitted to University of Benin in partial fulfillment of the requirements or the award of BSc is my original work. I have not submitted this work to any other institution for the award of any of any degree or diploma.

ACKNOWLEDEMENT

I would like to express my deepest gratitude to God Almighty for His divine guidance and strength throughout my academic journey.

My profound gratitude goes to my project supervisor, Prof. K.O. MUKA, his unwavering support enabled me to start and complete my project, his expert guidance, patience and valuable feedback throughout this project.

To the entire staff of Mathematics department, University of Benin, particularly my Course Advisers, Mrs I.J. Jacob, Dr (Mrs) R.U. Omoregie, Dr (Mrs) I.B. Aihie and Dr O.O. Olowu, thank you so much for your support and contribution to my academic growth.

My beloved mother, Augustine Obadoni, for her unwavering support, love, and encouragement. To my siblings, Rachael and Samuel, thank you so much for your love, care, and motivation.

To my wonderful cousins who made my stay in UNIBEN easy, Eloho, Elozino, Fejiro and Emmanuel, thank you so much.

Special appreciation to my aunt Veronica Oboh and her wonderful family for their kindness and support. Thank you so much, Mr and Mrs T. Omobah, Mrs Ishioma Daniel and her family, Mr Franklin Alegu and Sis Blessing Akpudje, God bless you.

Special thanks to all the pastors and the entire member at Zion Chapel, they have been of great help in every aspect of my life.

To my dear friends, Eloghosa, Precious, Peter, Fulness, Ifeoma, thank you so much for your motivation, and cherished memories.

Thank you all for being part of my academic journey!

DEDICATION

I dedicate this project to God Almighty.

ABSTRACT

The Dynamics of infectious diseases are vital in the disease control in populations. The mathematical methods that describe these diseases models often are insoluble hence, the need for numerical approximations

Stage two Runge-Kutta methods are used to integrate the system of differential equations that evolves in the model formulation of the infectious diseases being studied.

The stability analysis of Runge-Kutta method is done using boundary bars plot.

The solution and plots are carried out using MATHEMATICA program.

TABLE OF CONTENTS

APPENDIX

LIST OF TABLES

LIST OF FIGURES

Chapter 1

Introduction

1.0 Preamble

According to the World Health Organization, Infectious diseases represent a significant public health challenge worldwide, characterized by their ability to spread from one individual to another through various transmission mechanisms (World Health Organization [WHO], 2023). Infectious diseases are caused by pathogenic microorganisms such as bacteria, viruses, parasites, and fungi (WHO,2023). Unlike non-communicable diseases, the transmissible nature of infectious diseases enables them to spread rapidly through human population and other population of Interest. Potentially, causing widespread outbreaks, epidemics, or even pandemics (WHO, 2023).

Throughout history, infectious diseases have significantly impacted human populations, causing substantial morbidity and mortality. Examples include the flu, measles, Human Immunodeficiency Virus, strep throat, smallpox, influenza, tuberculosis, malaria, and more recently, Corona Virus-19.

1.1 Model used in Describing Infectious Diseases

Models used in describing Infectious Diseases can be Statistical or Mathematical models. Of the two, the Mathematical model as used in understanding dynamics that relates changes with time (Grassly and Fraser, 2008). Mathematical models have become indispensable tools in understanding the dynamics of infectious diseases and informing public health decision-making. These models provide a structured framework for conceptualizing the complex processes involved

in disease transmission and progression, allowing researchers to study the effects of various factors and interventions on disease spread within populations (Grassly and Fraser, 2008).

1.2 Mathematical Model

Mathematical model is an abstract representation of real-world phenomena, processes or systems using mathematical concepts and language, often expressed as equations or other mathematical expressions (Wikipedia,2025). A mathematical model uses the language of Mathematics to produce a more refined and precise description of a system (Wikipedia,2025). In epidemiology, models allow us to translate between behavior at various scales, or extrapolate from a known set of conditions to another (Hethcote, 2000).

Mathematical models serve multiple purposes in scientific inquiry:

1. They provide a framework for organizing and interpreting empirical data;
2. They allow for hypothesis testing and prediction of future states of the system;
3. They enable simulation of scenarios that might be impractical or unethical to conduct in real life;
4. They identify key variables and relationships that drive system behavior;
5. They facilitate the development and evaluation of intervention strategies.

In the context of infectious diseases, mathematical models translate biological processes into mathematical formulations that capture the essential dynamics of disease transmission and progression. These models range from simple deterministic equations to complex stochastic simulations involving numerous variables and parameters.

1.3 Advantages and Disadvantages

1. Mathematical models have become essential tools in infectious disease epidemiology and various other scientific fields. However, like any methodological approach, they have inherent strengths and limitations that must be carefully considered when developing, applying, and interpreting them (Keeling and Rohani, 2008; Brauer and Castillo-Chevez, 2012).

1.3.1 Advantages of Mathematical Models

1. **Formalization of Knowledge**: Mathematical models provide a rigorous framework for formalizing existing knowledge about a system, requiring explicit statement of assumptions and mechanisms that might otherwise remain implicit (Brauer and Castillo-Chevez, 2012).
2. **Optimization and Problem-Solving:** Mathematical Models can be used to identify optimal solutions for complex problems, considering various constraints and objectives. This is particularly useful in fields like engineering, finance and operation management.
3. **Prediction and Forecasting**: Mathematical models can generate predictions about future states of a system based on current conditions and understanding of underlying dynamics.
4. **Understanding Complex Systems**: Models help elucidate the behavior of complex systems where intuition alone may be insufficient, identifying emergent properties and non-linear effects that arise from interactions among system components (Keeling and Rohani, 2008).
5. **Identification of Knowledge Gaps**: The process of model development often reveals gaps in understanding or data, highlighting areas where further research is needed.

6. **Cost-Effectiveness**: Computational simulations are typically less expensive and time-consuming than large-scale field studies or experiments, allowing for exploration of multiple scenarios and sensitivity analyses.

1.3.2 Disadvantages of Mathematical Models

1. **Simplification of Reality**: Models necessarily simplify complex biological, social, and environmental processes, potentially omitting important factors or interactions that influence system behavior (Keeling and Rohani, 2008).
2. **Parameter Uncertainty**: Models often require parameters that may be difficult to estimate accurately from available data, introducing uncertainty into model predictions.
3. **Data Limitations**: The quality and quantity of data available for model development, calibration, and validation may be insufficient, especially for emerging diseases or understudied populations.
4. **Computational Constraints**: Complex models, particularly those with spatial heterogeneity, stochasticity, or individual-based components, may require substantial computational resources, limiting their practical application in some contexts.
5. **Validation Challenges**: Validating models of complex systems can be difficult, especially when modeling rare events, long-term processes, or counterfactual scenarios.

1.3.3 Balancing Trade-offs in Model Development

The development and application of mathematical models involves navigating trade-offs between simplicity and realism, generality and specificity, and theoretical insight and practical utility.

Finding the appropriate balance depends on the specific research question, available data, and intended use of the model.

For infectious disease modeling, Grassly and Fraser (2008) suggest considering five key questions when developing or evaluating a model:

1. What is the purpose of the model?
2. What is the appropriate level of complexity?
3. How can the model be validated?
4. How should uncertainty be incorporated and communicated?
5. How will the model be used to inform decisions?

By carefully considering these questions and acknowledging both the strengths and limitations of mathematical models, researchers can develop and apply models that provide valuable insights while avoiding potential pitfalls of misinterpretation or misapplication.

1.4 SIR Model

The most widely used approach to modeling infectious diseases involves compartmental models, which divide the population into distinct groups (compartments) based on their disease status. The simplest and most fundamental of these is the SIR model, introduced by Kermack and McKendrick in 1927, which categorizes individuals as:

1. **Susceptible (S)**: Individuals who have not been infected but are capable of contracting the disease and becoming infectious.

2. **Infectious (I)**: Individuals who have been infected and are capable of transmitting the disease to susceptible individuals.
3. **Recovered (R)**: Individuals who have recovered from the infection and are assumed to have developed immunity (or died), and therefore no longer participate in disease transmission.

The SIR model makes several key assumptions as noted by Keeling and Rohani (2008): These assumptions include:

1. The population size remains constant (no births, deaths, or migration)
2. The population is homogeneously mixed (all individuals have an equal probability of contact)
3. Individuals move from susceptible to infectious upon infection
4. Infected individuals move to the recovered compartment at a constant rate
5. Once recovered, individuals cannot be reinfected (permanent immunity)

While more sophisticated models exist that incorporate additional compartments (like SEIR, SIRS) or relax certain assumptions, the basic SIR model provides remarkable insights into epidemic dynamics while remaining mathematically tractable (Hethcote, 2000).

Solution is key to the understanding of all models formulations. This helps in policy formation of control of spread of disease in the populace. Absence of solution makes information diseases of dynamic of disease spread and establishment of equilibria point of the disease spread. As important as the solutions of mathematical models are, most models are insoluble, that is they do not possess

closed form solution. The problem of obtaining closed form solution results in the need for approximately solution (numerical solution).

1.5 Numerical Solution to Systems of equations

A Numerical method is a difference equation involving a number of consecutive approximations y_{n+j}, j = 0, 1, ..., k, from which it will be possible to compute sequentially the sequence $\{y_n \mid n = 0,1,2, \ldots, N\}$; naturally, this difference equation will also involve the function f. The integer k is called the step number of the method; if k = 1, the method is called one-step method, while if k >1, the method is called multistep or k-step (Burden and Faires, 2016).

The SIR model like other models of real-life phenomena is insoluble via analytically means, that is their solutions are not in closed form for arbitrary initial conditions. Numerical methods are essential for obtaining approximate solutions. Numerical methods discretize time and iteratively compute the state of the system at successive time points. Numerical methods produce particular solutions satisfying given initial and boundary value problems not systems.

Solution is key in the understanding of all model formulations. This helps in policy formation of control of spread of diseases in the populace. Absence of solution makes information decision of dynamics of disease spread and establishment of equilibrium point of the disease spread. As important as the solutions of mathematical model are, most models are insoluble, that is they do not possess closed form solution. The problem of obtaining closed form solutions results in the need for approximating solution (Numerical solution).

1.5.1 Need for Numerical Solutions

Mathematical Models are built using the tool of Differential Equations. SIR models are essentially system of Ordinary Differential Equations (ODEs). The SIR model forms a system of nonlinear differential equations that often cannot be solved explicitly analytically. While some special cases allow for analytical insights (such as early-stage approximations or equilibrium analysis), understanding the complete temporal dynamics of an epidemic typically requires numerical approximation.

1.5.2 Common Numerical Methods for ODEs

Several numerical methods exist for solving systems of Ordinary Differential Equations (ODEs), like the SIR model (Atkinson, K.E., 1989). The numerical methods are categorized into one-step or multistep methods.

One-step methods include:

1. Euler Method**:** The simplest numerical approach, which approximates solutions using first-order Taylor expansions. While straightforward to implement, it requires very small time steps for accuracy and can be unstable.
2. Runge-Kutta Methods**:** A family of iterative methods that offer improved accuracy compared to the Euler method. These methods evaluate the differential equations at multiple points within each time step to better approximate the solution curve.

Multistep Methods include:

1. Adams-Bashforth or Adams-Moulton that use information from multiple previous time steps to compute the next value.
2. Backward difference formula**:** approximates the derivates of a function at a point using the function's values at that point and a preceding point.

1.5.3 SOME BASIC DEFINITIONS

1.5.3.1 Convergence

A Numerical method converges if the approximate solution approaches the exact solution as we refine our computational parameters(Burden and Faires, 2016).

For a differential equation $\frac{dy}{dx} = f(t, y)$ with exact solution y(t), a numerical method with step size h converges if:

$$\lim_{h \to 0} |y_n - y(t_n)| = 0 \qquad (1.1)$$

Where y_n is the numerical approximation at time t_n.

Order of convergence: This tells us *how fast* we approach the exact solution. A method has order p if the global error behaves like O(h^p)**.** Higher order means faster convergence.

1.5.3.2 Stability

A numerical method is stable if small perturbations (errors) don't grow exponentially over time (Burden and Faires, 2016).

For the test equation $\frac{dy}{dx}$ = λy, where **λ < 0**, we want numerical solutions to decay like the exact solution y(t) = $y_0 e^{(\lambda t)}$.

Absolute stability region: The set of values hλ (where h is step size and λ is the eigenvalue) for which the method remains stable.

For Euler: $|1 + h\lambda| \leq 1$

A-stability: A method is A-stable if its stability region includes the entire left half-plane ($Re(h\lambda) \leq 0$). This is crucial for stiff equations.

1.5.3.3 Consistency

A numerical method is consistent if the local truncation error approaches zero as the step size decreases.

For a method approximating $\frac{dy}{dx} = f(t, y)$:

Local Truncation Error (LTE) $= [y(t_{n+1}) - y(t_n)]/ h - f(t_n, y(t_n))$

The method is consistent if:

$$\lim_{h \to 0} LTE = 0$$

Consistency + Stability = Convergence

1.5.3.4 Local and Global error

Local Error: The error made in a single step, assuming all previous values were exact.

Global Error: The total accumulated error after many steps.

Local error per step: $O(h\^\{p+1\})$

Global error after n steps: O(h^p**)** where n ≈ 1/h

1.5.3.5 Stiffness

A differential equation is stiff if it has solutions with vastly different time scales. Some components change very rapidly, others very slowly.

Mathematical indicator**:** Large negative eigenvalues in the system, or a large stiffness ratio:

Stiffness Ratio = $\max|Re(\lambda_i)|/\min|Re(\lambda_i)|$

Explicit methods require impractically small step sizes for stiff problems. Implicit methods are often necessary.

1.6 Problem Statement

Despite the widespread use of mathematical models in infectious disease epidemiology, there remains a significant challenge in efficiently obtaining accurate numerical solutions to these models, particularly in resource-constrained environments or when rapid results are needed for timely decision-making. While numerous numerical methods exist for solving systems of ordinary differential equations, there is limited systematic evaluation of the performance of Explicit Stage Two Runge-Kutta methods specifically for the SIR model of infectious diseases (Burden and Faires, 2016); Hethcote (2000).

This project addresses the following specific problems:

1. How do different variants of Explicit Stage Two Runge-Kutta methods compare in terms of accuracy and computational efficiency when applied to the SIR model of infectious diseases?
2. How do these numerical approximations perform under various epidemiological conditions, characterized by different values of the basic reproduction number (R_0) and initial conditions?
3. To what extent do numerical errors in these approximations affect key epidemiological insights, such as the timing and magnitude of the epidemic peak, the final size of the epidemic, and the threshold conditions for epidemic spread?

By addressing these questions, this project aims to provide practical guidance for researchers and public health practitioners on the appropriate application of Explicit Stage Two Runge-Kutta methods for SIR models, contributing to more reliable epidemic forecasting and intervention planning.

1.7 Aim and Objective

1.7.1 Aim

The aim of this project is to carry out survey of Susceptible Infected Recovered (SIR) models for Infectious Diseases using Explicit Stage Two Runge-Kutta processes.

1.7.2 Objectives

The specific objectives of this project are:

1. Determine efficient methods amongst Explicit Runge-Kutta stage methods for integrating system of SIR model
2. Formulate and analyze mathematical models for three infectious diseases using SIR models.
3. Develop and implement Explicit Stage Two Runge-Kutta numerical schemes for approximating solutions to these models.
4. Evaluate the accuracy and efficiency of the numerical schemes for each disease model.
5. Compare the approximate solutions with analytic solutions (where possible) and discuss the implications of the results.

The findings will help ensure that the insights derived from SIR models are based on numerically sound approximations, ultimately supporting more effective infectious disease control and prevention strategies.

1.8 Summary and Conclusion

This introductory chapter has established the foundation for our investigation into the application of Explicit Stage Two Runge-Kutta processes for obtaining approximate solutions to the SIR model of infectious diseases. We began by defining infectious diseases and their significance in public health, highlighting the need for Mathematical modeling to understand and predict the spread of infectious diseases in human population.

In the subsequent chapters, we will systematically address these objectives, beginning with a detailed exposition of the Explicit Stage Two Runge-Kutta methods and their application to the SIR model. We will then present our methodology for evaluating these methods, analyze the

results of our numerical experiments, and conclude with recommendations for their optimal application in different contexts.

Chapter 2

Mathematical Models for Infectious Diseases

2.1 Introduction

The Susceptible-Infected-Recovered (SIR) model, as introduced in Chapter 1, provides a fundamental framework for understanding the dynamics of infectious disease transmission. While the mathematical elegance of the SIR model is universally applicable, its real-world implementation requires careful consideration of disease-specific characteristics, population dynamics, and local epidemiological contexts. In Nigeria, a country with a population exceeding Two Hundred and Twenty Million (220,000,000) people and diverse ecological zones, infectious diseases remain a significant public health challenge, contributing substantially to morbidity and mortality rates across all age groups.

Nigeria's unique epidemiological landscape presents both opportunities and challenges for mathematical modeling of infectious diseases. The country's tropical climate, varying population densities, diverse socioeconomic conditions, and existing healthcare infrastructure create complex transmission dynamics that can be effectively captured through appropriately parameterized SIR models. Understanding these dynamics is crucial for public health planning, resource allocation, and the development of effective intervention strategies.

This chapter focuses on three infectious diseases that are particularly relevant to the Nigerian context and can be effectively modeled using SIR frameworks: measles, influenza, and Lassa fever. Each of these diseases represents different transmission characteristics, population impacts,

and public health priorities, making them ideal candidates for demonstrating the versatility and applicability of SIR models in diverse epidemiological settings.

The selection of these diseases is based on several criteria: their significant burden on the Nigerian population, availability of epidemiological data, distinct transmission patterns that showcase different aspects of SIR modeling, and their relevance to current public health policy and intervention strategies. By examining these diseases through the lens of mathematical modeling, valuable insights into their transmission dynamics and inform evidence-based decision-making for disease control and prevention can be realized.

2.2 Infectious Diseases

Infectious Diseases such as Measles, Influenza and Lassa fever have been modeled as SIR model. The choice of Measles, Influenza, and Lassa fever for this study represents a strategic selection that captures the breadth of infectious disease challenges facing Nigeria. These diseases span different transmission modes, seasonal patterns, geographic distributions, and public health impacts, providing a comprehensive foundation for public health management. The Explicit RK method will be used to help in model validation through iterative production and numerical approximations.

2.2.1 Measles

Measles represents a classic example of a highly contagious vaccine-preventable disease with well-documented transmission parameters. Despite the availability of an effective vaccine, measles continues to cause significant outbreaks in Nigeria, particularly in areas with low

vaccination coverage. The disease's high basic reproduction number (R_0) and clear seasonal patterns make it an excellent candidate for SIR modeling.

2.2.2 Influenza

Influenza exemplifies seasonal respiratory infections with complex transmission dynamics influenced by viral evolution, seasonal patterns, and varying population immunity. In Nigeria, influenza circulation patterns are influenced by the country's position in the tropical belt, with transmission occurring year-round but with distinct seasonal peaks corresponding to the harmattan and rainy seasons.

2.2.3 Lassa fever

represents an emerging infectious disease with zoonotic origins, endemic to West Africa, including Nigeria. Unlike the other two diseases, Lassa fever has a more complex transmission pattern involving both human-to-human transmission and zoonotic transmission from rodent reservoirs. This disease showcases the adaptability of SIR models to capture endemic diseases with sustained transmission in specific geographic regions.

Each of these diseases provides unique insights into different aspects of infectious disease transmission and demonstrates the flexibility of SIR models in capturing diverse epidemiological phenomena. The mathematical frameworks developed for these diseases can serve as templates for modeling other infectious diseases with similar transmission characteristics.

2.3 MATHEMATICAL MODELS

In this section, mathematical models of Measles, Influenza and Lassa Fever is categorized into Diseases A, B and C respectively.

2.3.1 Disease A: Measles

Measles remains one of the leading causes of vaccine-preventable deaths globally, and Nigeria has consistently been among the countries with the highest burden of measles cases. According to the World Health Organization (WHO, 2023), Nigeria accounted for approximately 20% of global measles deaths in recent years, with children under five years of age being disproportionately affected. The disease is caused by the measles virus (MeV), a highly contagious paramyxovirus that spreads through respiratory droplets and aerosols.

In the Nigeria measles transmission is characterized by several distinctive features. The disease exhibits strong seasonal patterns, with peak transmission typically occurring during the dry season (November to April) when population density increases due to reduced agricultural activity and increased indoor gatherings. The harmattan winds during this period may also facilitate aerosol transmission over longer distances. Additionally, the timing of outbreaks often coincides with the period following the rainy season when malnutrition rates may be elevated, potentially increasing both susceptibility to infection and severity of disease outcomes.

The Nigerian healthcare system's response to measles has evolved significantly over the past decades. Routine immunization programs, supplemented by periodic mass vaccination campaigns, have achieved variable coverage across different states and regions. Northern states, particularly those affected by security challenges and nomadic populations, have historically experienced

lower vaccination coverage rates, creating pockets of susceptible individuals that can sustain transmission and trigger outbreaks.

The SIR model for measles in Nigeria can be formulated as a system of ordinary differential equations that capture the essential dynamics of measles transmission:

2.3.1.1 System of Differential Equations

The measles model shows the simplest disease flow with two transitions:

S to I: Susceptible people get infected when they contact infectious people (rate: βSI/N)

I to R: Infected people recover and gain permanent immunity (rate: γI)

Once recovered, people cannot get measles again. This creates a one-time epidemic that burns through the population and ends when susceptible people are exhausted.

Figure 2.1: Schematic Diagram for SIR model of Measles

The population is assumed fixed herein, that is total population is N. it is assumed that the entire population can be placed in the compartments such as susceptible, infected, recovered. That is at every time t, the total number of persons in susceptible, infected and recovered class sums up to N. The schematic diagram is shown in figure2.1

$$\left.\begin{aligned} \frac{dS}{dt} &= \frac{-\beta SI}{N} \\ \frac{dI}{dt} &= \frac{\beta SI}{N} - \gamma I \\ \frac{dR}{dt} &= \gamma I \end{aligned}\right\} \quad (2.1)$$

Where:

S(t) = Number of susceptible individuals at time t

I(t) = Number of infectious individuals at time t

R(t) = Number of recovered individuals at time t

N = Total population size (S + I + R = N)

β = Transmission rate parameter

γ = Recovery rate parameter (1/γ = infectious period)

Model Parameters for Measles: The parameterization of the measles SIR model for Nigeria requires consideration of local epidemiological characteristics:

1. Basic Reproduction Number (R_0): For measles, R_0 values typically range from 12-18, reflecting the highly contagious nature of the virus. This value may vary seasonally and

geographically, with higher values observed during dry season outbreaks and in areas with high population density.

2. Infectious Period ($1/\gamma$): The infectious period for measles is typically 8-9 days, and they start feeling better within 7-10 days (WHO). This parameter is relatively consistent across populations but may be influenced by nutritional status and concurrent infections.
3. Transmission Rate (β): β = (number of new infections)/ (number of contacts between infectious and susceptible individuals). The transmission rate β can be calculated as $\beta = R_0 \times \gamma$, but it may exhibit seasonal variation due to factors such as school calendars, religious gatherings, and environmental conditions.

2.3.2 Disease B: Influenza

Influenza represents a significant respiratory disease burden in Nigeria, with circulation patterns that differ markedly from temperate regions. In tropical and subtropical regions like Nigeria, influenza transmission occurs year-round with distinct seasonal peaks that coincide with specific climatic conditions. The Nigeria Centre for Disease Control (NCDC) surveillance data indicates that influenza activity typically peaks during two distinct periods: the harmattan season (December-February) and the early rainy season (May-July).

The epidemiology of influenza in Nigeria is characterized by the circulation of multiple virus types and subtypes, including seasonal influenza A (H1N1 and H3N2) and influenza B viruses. The antigenic evolution of these viruses, combined with waning immunity from previous infections and vaccinations, creates complex transmission dynamics that challenge traditional SIR modeling approaches. However, for the purposes of this study, we focus on single-strain dynamics that can be effectively captured by modified SIR models.

Nigeria's position in West Africa makes it a crucial junction for influenza virus circulation between different regions. The country's large population, significant internal migration patterns, and connections to global transportation networks create conditions that facilitate both local transmission and the introduction of new viral variants. Understanding these dynamics is essential for pandemic preparedness and seasonal influenza control strategies.

The burden of influenza in Nigeria extends beyond direct health impacts to include significant economic consequences. Healthcare system strain during peak transmission periods, productivity losses due to illness, and the costs of preventive measures all contribute to the overall societal impact of influenza. Mathematical modeling can help quantify these impacts and guide resource allocation decisions.

The SIR model for influenza requires modifications to account for several unique characteristics of the disease.

2.3.2.1 Basic SIR System

The influenza model adds a third transition creating a cycle:

S to I: Infection occurs through contact (rate: $\beta SI/N$)

I to R: Recovery with temporary immunity (rate: γI)

R to S: Immunity wanes, people become susceptible again (rate: ωR)

Key characteristic: The return flow from R to S allows repeated epidemics. People can get influenza multiple times as their immunity fades. The key difference is that immunity wanes (rate ωR), allowing people to become susceptible again. This creates repeating epidemic cycles.

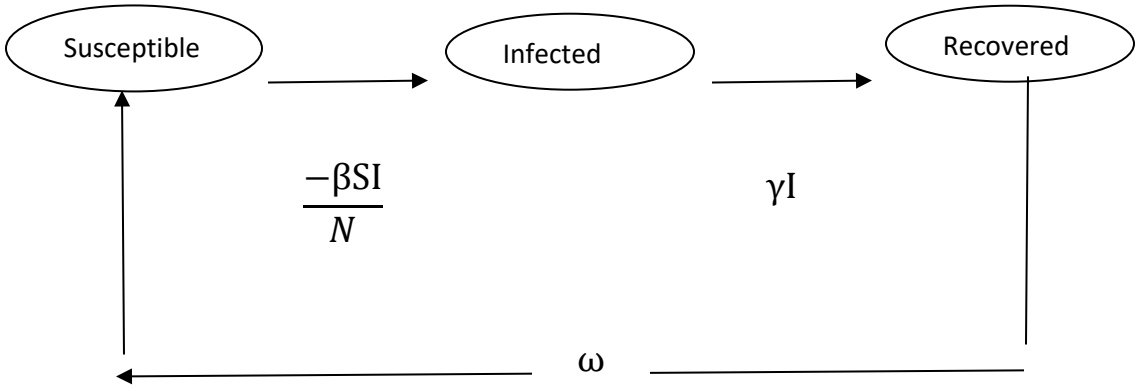

Figure 2.2: Schematic Diagram for SIR model of Influenza

$$\left.\begin{aligned} \frac{dS}{dt} &= \frac{-\beta SI}{N} + \omega R \\ \frac{dI}{dt} &= \frac{\beta SI}{N} - \gamma I \\ \frac{dR}{dt} &= \gamma I - \omega R \end{aligned}\right\} \qquad (2.2)$$

The key modification is the inclusion of the waning immunity term (ωR), which accounts for the temporary nature of influenza immunity. This creates a SIRS (Susceptible-Infected-Recovered-Susceptible) model that better captures the recurrent nature of influenza epidemics.

Parameter Specifications for Influenza

1. Basic Reproduction Number (R_0)**:** For seasonal influenza, R_0 typically ranges from 1.2-1.8, significantly lower than measles but sufficient to sustain transmission in susceptible populations.
2. Infectious Period ($1/\gamma$)**:** The infectious period for influenza is approximately 3-7 days, giving $\gamma \approx 0.14\text{-}0.33$ per day.
3. Immunity Waning Rate (ω): The rate of immunity loss varies by virus type and individual factors, but for seasonal influenza, immunity typically wanes over 1-3 years, giving $\omega \approx 0.001\text{-}0.003$ per day.

2.3.3 Disease C: Lassa Fever

Lassa fever represents a unique challenge in the Nigerian infectious disease landscape as an endemic viral hemorrhagic fever caused by the Lassa virus (LASV). First identified in Lassa, Borno State, Nigeria in 1969, the disease has since been recognized as a significant public health threat across West Africa, with Nigeria bearing the highest burden of cases globally. The Nigeria Centre for Disease Control (NCDC) reports in 2024 confirmed 857 cases of Lassa fever and 156 deaths across 28 states. States like Ondo, Edo, and Bauchi have been particularly affected, accounting for 63% of the confirmed cases in 2024.

The epidemiology of Lassa fever is characterized by its endemic nature in specific geographic regions, primarily the Middle Belt and Northern states of Nigeria. The disease exhibits a complex transmission pattern involving both zoonotic transmission from the multimammate rat (Mastomys natalensis) reservoir and human-to-human transmission through contact with bodily fluids of infected individuals (blood, urine, feces, vomits etc.), particularly in healthcare settings and among

family members providing care to infected individuals. Transmission always occurs through contact with rat's urine and feces, or by touching contaminated objects, food, or open wounds.

Seasonal patterns of Lassa fever in Nigeria correspond closely to the agricultural calendar and climatic conditions. Peak transmission typically occurs during the dry season (November-April) when contact between humans and rodent reservoirs increases due to agricultural activities, food storage practices, and environmental factors that drive rodents into human habitations. The harmattan winds may also contribute to the dispersal of contaminated rodent excreta, facilitating environmental transmission.

The healthcare system's response to Lassa fever has improved significantly since the establishment of dedicated treatment centers and enhanced surveillance systems. However, challenges remain in early case detection, appropriate case management, and infection prevention and control in healthcare settings. The case fatality rate varies widely, from less than 1% in mild cases to over 15% in severe cases, highlighting the importance of early detection and appropriate clinical management.

2.3.3.1 SIR for Lassa Fever

The SIR model for Lassa fever requires consideration of the disease's unique transmission characteristics. Lassa fever disease is known to ultimately progress to death of individuals effected. This is identified in the schematic diagram as shown in figure 2.3

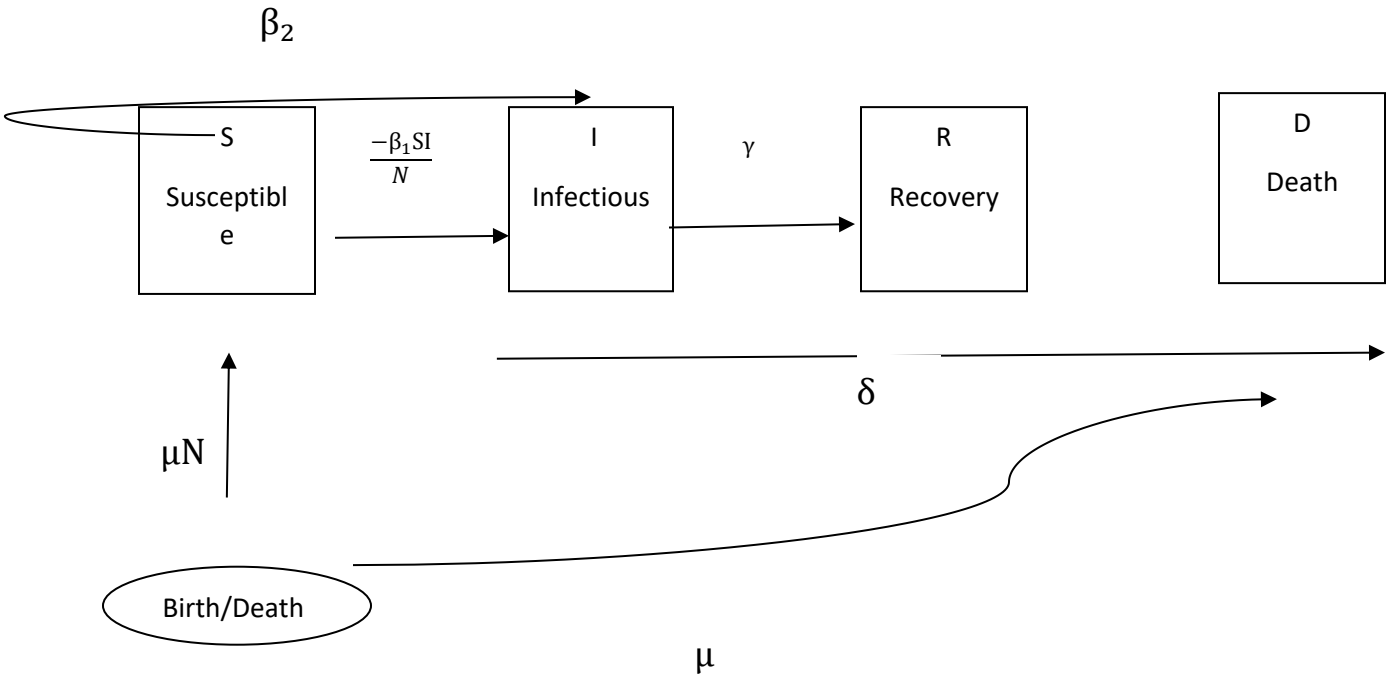

Figure 2.3: Schematic Diagram for SIR model of Lassa Fever

Multiple pathways in and out:

People enter as susceptible through births (μN)

Two infection routes: human contact ($\beta_1 SI/N$) and environmental exposure to rodents ($\beta_2 S$)

Three exit routes from infected: recovery (γI), disease death (δI), or natural death (μI)

Natural death removes people from all compartments (μS, μR)

$$\left.\begin{aligned} \frac{dS}{dt} &= \frac{-\beta_1 SI}{N} - \beta_2 S + \mu N - \mu S \\ \frac{dI}{dt} &= \frac{\beta_1 SI}{N} + \beta_2 S - (\gamma + \delta + \mu)I \\ \frac{dR}{dt} &= \gamma I - \mu R \\ \frac{dD}{dt} &= \delta I \end{aligned}\right\} \quad (2.3)$$

Where:

β_1 = Human-to-human transmission rate

β_2 = Zoonotic transmission rate (environmental exposure)

δ = Disease-induced mortality rate

μ = Natural birth/death rate

D = Cumulative deaths

Parameter Specifications for Lassa Fever

1. Basic Reproduction Number (R_0): For Lassa fever, R_0 estimates range from 1.1-1.8(Wang et al (2021)), varying by geographic region and season. The value incorporates both human-to-human and zoonotic transmission components.
2. Infectious Period ($1/\gamma$)**:** The incubation period of Lassa fever ranges from 2–21 days (WHO,2024).

3. Case Fatality Rate ($\delta/(\gamma+\delta)$)**:** The overall case fatality rate is 1% but observed case fatality rate among patients hospitalized with severe diseases of Lassa fever is 15% and above (WHO,2024).
4. Zoonotic Force of Infection (β_2)**:** This parameter captures environmental exposure risk and varies seasonally and geographically based on rodent population dynamics and human-rodent contact patterns.

2.4 Summary

This chapter has provided a comprehensive overview of three infectious diseases that can be effectively modeled using SIR frameworks in the Nigerian context. Measles, influenza, and Lassa fever each present unique characteristics that demonstrate the versatility and adaptability of SIR models for capturing diverse transmission dynamics.

The mathematical formulations presented for each disease provide the foundation for implementing Explicit Stage Two Runge-Kutta numerical methods, which will be the focus of subsequent chapters. The availability of diverse data sources for each disease enables robust model parameterization and validation, supporting the practical application of these mathematical frameworks for public health decision-making.

In the next chapter, we will detail the specific Explicit Stage Two Runge-Kutta methods that will be applied to these disease models, providing the numerical foundation for obtaining approximate solutions to these complex epidemiological systems.

Chapter 3

Numerical Methods

3.1 Introduction

The theoretical framework for understanding disease transmission dynamics is easily established through Mathematical models of the diseases they represent. However, the practical application of these models requires robust numerical methods to obtain approximate solutions, particularly when analytical solutions are either unavailable or computationally intractable. This chapter focuses on the implementation and analysis of Explicit Stage Two Runge-Kutta methods for solving the Ordinary Differential Equation systems that evolve from Mathematical Models of measles, influenza, and Lassa fever transmission.

The complexity inherent in infectious disease modeling stems from the nonlinear nature of the differential equations and the interdependence of the compartments within each model, while the SIR framework provides an elegant mathematical representation of disease transmission, the coupled nature of the differential equations prevents closed-form analytical solutions for most realistic parameter combinations and initial conditions (Brauer and Castillo-Chavez,2012).

Numerical approximation methods help in the validation of models and their practical applications. Of the various numerical schemes available for integrating Ordinary Differential Equations, the Explicit Stage Two Runge-Kutta methods offer an optimal balance between computational efficiency and numerical accuracy. These methods are particularly well-suited for epidemiological applications where timely results are essential for public health decision-making (Burden and Faires, 2016).

The choice of numerical method significantly impacts the reliability of model predictions and, consequently, the effectiveness of public health interventions based on these predictions. Therefore, understanding the properties, strengths, and limitations of different numerical schemes is crucial for epidemiologists and public health practitioners who rely on mathematical models for policy guidance.

A systematic examination of the basic properties of each disease model developed, appropriate numerical schemes required for the solution of these models which will help in providing analytical insights shall be highlighted. Analysis will be carried out to demonstrate, how numerical methods can be tailored to the specific characteristics of different infectious diseases in this study while maintaining computational efficiency and solution accuracy.

3.2 Basic Properties

The SIR model serves as a fundamental tool for understanding how infectious diseases spread through populations (Kermack and McKendrick, 1927). This formalism, which was initially studied in depth by Kermack and McKendrick (1927), categorizes hosts within a population as Susceptible (if previously unexposed to the pathogen), Infected (if currently colonized by the pathogen), and Recovered (if they have successfully cleared the infection).

Understanding the fundamental properties of infectious disease models is essential for selecting appropriate numerical methods and interpreting simulation results. Each disease model exhibits unique characteristics that influence both the choice of numerical scheme and the interpretation of results (Keeling and Rohani (2008). These fundamental mathematical properties of SIR model is crucial for epidemiologists and public health practitioners who rely on these models for disease

control strategies and policy decisions. This section provides an in-depth exploration of three cornerstone concepts that govern the behavior of infectious disease models: equilibrium analysis, stability analysis, and threshold phenomena.

These properties provide insights into long-term disease behavior, identify conditions for epidemic emergence, and establish bounds on solution trajectories. For numerical methods, these properties serve as validation criteria and help identify potential sources of computational error.

3.2.1 Threshold Phenomena

Perhaps no concept in mathematical epidemiology has garnered as much attention and practical application as the threshold phenomenon governed by the basic reproduction number R_0 (Diekmann, O., Heesterbeek, J. A. P., and Roberts M.G. (2010). There is hardly a paper on dynamic epidemiological models in the literature where R_0 does not play a role. R_0 is defined as the average number of new cases of an infection caused by one typical infected individual, in a population consisting of susceptible only.

3.2.1.1 The Basic Reproduction Number(R_0)

The basic reproduction number represents the average number of secondary infections produced by a single infected individual in a completely susceptible population during their entire infectious period. This seemingly simple definition carries profound implications for understanding disease transmission and designing control strategies.

It is defined as the expected number of secondary infections that would generate by a typical infected case in a wholly susceptible population. For the basic SIR model, $R_0 = \beta/\gamma$, where β represents the transmission rate and γ represents the recovery rate.

3.2.1.2 The Threshold Condition

The threshold phenomenon manifests through a critical condition that determines whether an infectious disease can invade and persist in a population. The basic reproduction number is a threshold: when it is less than unity the disease-free equilibrium exists and is stable, which indicates that the disease will die out; when it is greater than unity the disease-free equilibrium becomes unstable, allowing for disease persistence.

This threshold behavior can be understood intuitively:

$R_0 < 1$: Each infected person, on average, infects fewer than one other person, causing the infection to eventually die out

$R_0 = 1$: The infection maintains itself at a constant level (critical threshold)

$R_0 > 1$: Each infected person infects more than one other person on average, leading to epidemic growth

3.2.1.3 Practical Implications of Threshold Phenomena

Understanding threshold phenomena provides actionable insights for public health decision-making:

Vaccination Strategies: The critical vaccination coverage required to prevent epidemics is directly related to R_0. The herd immunity threshold is calculated as $1 - 1/R_0$, meaning that approximately 93% of the population must be immune to prevent sustained transmission.

Control Measure Effectiveness: Interventions such as social distancing, improved hygiene, or case isolation can be evaluated by their impact on reducing R_0 below unity. This provides a quantitative framework for assessing policy effectiveness.

Seasonal and Environmental Factors: Understanding how environmental conditions, population density, and social behaviors influence R_0 helps predict seasonal epidemic patterns and geographic variations in disease transmission.

3.2.2 Equilibrium Analysis

Equilibrium analysis in epidemiological modeling seeks to identify the steady-state conditions where the rates of change in each compartment become zero. These equilibrium points represent the long-term behavior of disease transmission dynamics and provide critical insights for public health planning.

Mathematical Foundation of Equilibrium Points

In mathematical terms, equilibrium occurs when all derivatives in the system equal zero simultaneously:

$$\frac{dS}{dt} = \frac{dI}{dt} = \frac{dR}{dt} = \frac{dD}{dt} = 0 \qquad (3.1)$$

For any SIR system, this condition leads to identifying specific combinations of susceptible, infected, and recovered populations that remain constant over time. The significance of these

points extends beyond mathematical curiosity—they represent realistic scenarios that epidemiologists encounter in practice.

1. **Disease-Free Equilibrium**: The disease-free equilibrium represents a state where the infectious disease has been completely eliminated from the population. Classical susceptible-infectious-recovered (SIR) models with a bilinear incidence rate usually have a disease-free equilibrium and at most one endemic equilibrium.

   Mathematically, this is represented as (S*, I*, R*) = (N, 0, 0), where the entire population consists of susceptible individuals with no infected or recovered persons present.

   This equilibrium point is particularly relevant for eradication campaigns, such as the successful global smallpox eradication program or ongoing efforts to eliminate measles in various regions. Understanding when and how a population can achieve and maintain this state is fundamental to designing effective public health interventions.

2. **Endemic Equilibrium**: The endemic equilibrium describes a state where the disease persists indefinitely within the population at stable levels. Unlike epidemic outbreaks that show dramatic rises and falls in case numbers, endemic diseases maintain relatively constant transmission rates over extended periods. SIR model is one of the classical epidemic models with compartment structure, suitable for the transmission of infectious diseases that confer long-lasting immunity such as chicken pox and SARS.

   For the basic SIR model with vital dynamics (births and deaths), the endemic equilibrium exists when:

$S^* = 1/R_0$ (the fraction of susceptible equals the inverse of the basic reproduction number)

$I^* = \mu(R_0 - 1)/\beta$ (the infected population depends on the birth rate, reproduction number, and transmission rate)

$R^* = \gamma I^*/\mu$ (the recovered population is proportional to the infected population)

This equilibrium only exists when $R_0 > 1$, highlighting the fundamental role of the reproduction number in determining disease persistence.

3.2.3 Stability Analysis

Stability analysis examines how the system responds when small changes or disturbances occur near equilibrium points. This analysis is crucial because real-world populations constantly experience fluctuations due to various factors including seasonal variations, policy changes, demographic shifts, or random events. Understanding stability helps predict whether these perturbations will grow (leading to instability) or decay (maintaining stability).

(i) Local Stability Analysis: Local stability analysis focuses on the behavior of the system in the immediate vicinity of equilibrium points. The existence and stability of the possible equilibria are examined in terms of a certain threshold condition. This analysis typically involves linearizing the nonlinear differential equations around the equilibrium point and examining the eigenvalues of the resulting Jacobian matrix.

For the disease-free equilibrium, local stability depends critically on whether R_0 is less than or greater than one:

When $R_0 < 1$: The disease-free equilibrium is locally asymptotically stable, meaning small introductions of infected individuals will not lead to sustained transmission

When $R_0 > 1$: The disease-free equilibrium becomes unstable, indicating that disease introduction can lead to epidemic growth

(ii) Global Stability Analysis: While local stability provides insights about behavior near equilibrium points, global stability analysis examines the system's behavior throughout the entire phase space. When $R_0 < 1$, the disease-free steady state is locally stable, which implies that the disease is extinct, when $R_0 > 1$, the disease is permanent, and there exists at least one positive steady state solution.

Global stability results are particularly valuable because they provide assurance that the predicted long-term behavior holds regardless of initial conditions. For epidemiological applications, this means that control strategies based on stability analysis remain valid across different outbreak scenarios and population compositions.

3.2.4 Threshold for Infectious Disease

The threshold phenomena principles apply directly to the three diseases examined in this study:

(i) Measles (Disease A)**:** With R_0 values ranging from 12-18, measles exhibits strong threshold behavior. The high reproduction number explains why measles outbreaks can occur even in populations with moderately high vaccination coverage, emphasizing the need for sustained high-coverage immunization programs.

(ii) Influenza (Disease B)**:** The lower R_0 values (1.2-1.8) for seasonal influenza create different threshold dynamics. The proximity to the critical threshold means that relatively modest interventions can potentially prevent epidemic spread, but the waning immunity component complicates long-term control strategies.

(iii) Lassa Fever (Disease C)**:** The intermediate R_0 values (1.2-2.1) and dual transmission pathways (human-to-human and zoonotic) create complex threshold behaviors that vary seasonally and geographically, reflecting the intricate relationship between human populations and rodent reservoirs.

3.2.5 DISEASE DYNAMICS

These three analytical frameworks work synergistically to provide a comprehensive understanding of disease dynamics. The threshold phenomenon determines which equilibria are biologically feasible, stability analysis predicts whether these equilibria are attainable and maintainable, and equilibrium analysis provides the mathematical foundation for long-term predictions.

For numerical methods implementation, these properties serve as crucial validation criteria. Numerical solutions must preserve the fundamental relationships between R_0 and equilibrium stability, maintain population conservation laws where appropriate, and accurately capture threshold transitions. Any numerical scheme that violates these fundamental properties would produce unreliable predictions, potentially leading to misguided public health decisions.

The mathematical rigor underlying these concepts ensures that epidemiological models remain grounded in sound theoretical foundations while providing practical tools for real-world applications. As we progress to implement and compare different numerical methods for solving

these models, the principles established through equilibrium analysis, stability analysis, and threshold phenomena will serve as our guiding framework for evaluating solution accuracy and biological realism.

3.3 Numerical Schemes for Approximating Solutions

A mathematical technique known as a numerical method is used to find approximate solutions to problems that are hard or impossible to solve analytically (with precise formulas) (Burden and Fairies (2016). Instead of providing precise symbolic answers, these approaches generate numerical approximations using computational algorithms.

$$y_{n+j}, \qquad j = 0,1,\ldots,k$$

where k is called the step length. It is called one-step method if k = 1 and multistep method if k>1 The general form of one-step and multistep methods is given as

$$\sum_{j=1}^{s} a_j y_{n+j} = h\,\phi_f\,(x_n, y_n + \mathrm{k}, y_n + \mathrm{k} - 1, \ldots, y_n, \mathrm{h})$$

One-step method is given as

$$y_{n+1} = y_n + h_n \phi_f\,(t_n, y_n;\ h_n) \qquad (3.2)$$

where

h_n is the step size adopted in the subinterval (t_n, t_{n+1}),

$\phi(t_n, y_n; h_n)$ is the increment function.

The simplest of all numerical methods is the Euler's Method, given as:

$$y_{n+1} = y_n + hf_n \tag{3.3}$$

It is linear in y_n and f_n and, being a one-step method, presents no difficulty when we want to change the step length; but of course, it has very low accuracy.

By maintaining linearity with regard to f_{n+j}, = j = 0,1,..., k, while forgoing the one-step format, linear multistep methods attain greater accuracy. The local error has a relatively simple structure as a result of maintaining linearity, which is why we can estimate it so easily by combining two methods to more approximate the error in each step to ensure that the solution stays within a given error tolerance.

As we have seen, the cost of switching to a multistep format is the significant challenges we face when attempting to alter step length.

Euler's Rule is the foundation of Runge-Kutta methods, which preserve the one-step form while sacrificing linearity to achieve higher order. Runge-Kutta methods were developed to preserve computational viability while overcoming the drawbacks of more straightforward strategies, such as Euler's method (Akhinson(1989)); (Butcher, J.C. (2003)).

The general s-stage Runge-Kutta method for solving initial values problem:

$$y' = f(x,y), y(t_0) = y_0 \tag{3.4}$$

Is given by:

$$y_{n+1} = y_n + h \sum_{i=1}^{s} b_i k_i \qquad (3.5)$$

Where the s-stage k_i are computed as:

$$k_i = f(t_n + c_i h, y_n + h \sum_{j=1}^{s} a_{ij} k_j), \qquad i = 1, 2, \ldots, s \qquad (3.6)$$

Assuming that the row-sum condition holds:

$$c_i = \sum_{j=1}^{s} a_{ij}, \qquad i = 1, 2, \ldots, s \qquad (3.7)$$

3.3.1 Classification of Runge-Kutta Method

Runge-kutta method can be grouped into three(3) categories which are:

(i) **Explicit method**: Explicit Runge-Kutta methods compute the solution at the next time step based solely on values from the previous time step(s). In explicit RK methods, the matrix A in the Butcher tableau is **strictly lower triangular** (a_{ij} = 0 for j ≥ i). Each stage k_i depends only on previously computed stages k_1, k_2, ..., k_{i-1}. Computationally efficient. Generally have stability restrictions (smaller step sizes required).

$$k_i = f(t_n + c_i h, y_n + h\sum_{j=1}^{i-1} a_{ij}k_j), \quad i = 1,2,\ldots,s$$
$$a_{ij} = 0, j \geq i, for\ j = 1,2,\ldots,s \qquad (3.8)$$

(ii) **Implicit method**: Implicit methods require solving an equation to determine the solution at the next time step. In implicit RK methods, the matrix A has **non-zero entries above or on the diagonal** (at least one $a_{ij} \neq 0$ for j ≥ i). Stages k_i may depend on each other, including themselves. Requires solving a (generally nonlinear) system of equations at each step. Better stability properties (can use larger step sizes).

$$k_i = f(t_n + c_i h, y_n + h\sum_{j=1}^{s} a_{ij}k_j),\ i = 1,2,\ldots,s$$
$$a_{ij} \neq 0, for\ some\ j > i \qquad (3.9)$$

(iii) **Semi-implicit method**: Semi-implicit method combines elements of explicit and implicit

$$a_{ij} = 0, for\ some\ j > i$$

3.3.2 Butcher Tableau

The Butcher tableau is a compact way to represent RK methods using coefficients:

c_1	a_{11}	a_{12}	...	a_{1s}
c_2	a_{21}	a_{22}	...	a_{2s}
⋮	⋮	⋮	⋱	⋮
c_s	a_{s1}	a_{s2}	...	a_{ss}
	b_1	b_2	...	b_s

Components:

c_i: Nodes (time points where function evaluations occur)

a_{ij}: Coupling coefficients between stages

b_i: Weights for final combination

3.3.3 General Explicit Stage Two Runge-Kutta Framework

For a stage two explicit Runge-Kutta method is a numerical method for approximating the solution of Ordinary Differential Equations (ODEs). It uses two intermediate steps (stages) within each time step to improve accuracy compared to simpler method like Euler's method. These methods are explicit because the solution at the next time step is calculated directly from the current and previous time steps, without needing to solve a system of equations.

For a general system of differential equations $\frac{dy}{dt}$ = f(t, y), the Explicit Stage Two Runge-Kutta method takes the form:

Stage 1: $k_1 = hf(t_n, y_n)$

Stage 2: $k_2 = hf(t_n + c_2h, y_n + a_{21}k_1)$

Update: $y_{n+1} = y_n + h(b_1k_1 + b_2k_2)$

where:

t_n and y_n are the current values of x and y;

h is the step size;

k_1 and k_2 are intermediate values calculated at different points within the interval (t_n, t_{n+1});

a_{21} determines how much of the previous stage's value (k_1) is used in calculating k_2;

c_2 determines the t-value at which k_2 is evaluated.

b_1, and b_2 are coefficients that determine the specific method.

The specific values of the parameters a_{21}, b_1, b_2, and c_2 determine the particular variant of the RK2 method.

$$y_{n+1} = y_n + h\sum_{i=1}^{2} b_i k_i \qquad (3.10)$$

$$k_i = f(t_n + c_i\, h,\quad y_n + h\sum_{j=1}^{2} a_{ij}k_j),\qquad i = 1,2 \tag{3.11}$$

(3.10) and (3.11) can easily be expressed as Butcher array

c_1	a_{11}	a_{12}
c_2	a_{21}	a_{22}
	b_1	b_2

Now, consider the initial value problem:

$\frac{dy}{dt} = f(t,y), y(t_0) = y_0$

All second-order Runge-Kutta methods have the general form:

$$\left.\begin{aligned} y_{n+1} &= y_n + h(b_1k_1 + b_2k_2) \\ k_1 &= hf\,(t_n, y_n) \\ k_2 &= hf\,(t_n + c_2h, y_n + a_{21}k_1) \end{aligned}\right\} \tag{3.12}$$

The most general explicit two-stage RK method has the Butcher tableau:

0	0	0
c_2	a_{21}	0

	b_1	b_2

where $c_2 = a_{21}$ (consistency condition).

Algorithm:

Given y_n at time t_n, compute y_{n+1} at time $t_{n+1} = t_n + h$:

$$y_{n+1} = y_n + h(b_1 k_1 + b_2 k_2)$$

where

$$k_1 = hf\ (t_n, y_n)$$

$$k_2 = hf\ (t_n + c_2 h, y_n + a_{21} k_1)$$

Parameter Relationships:

For a method of order $p \geq 2$, we need:

Order 1: $b_1 + b_2 = 1$

Order 2: $b_2 c_2 = 1/2$

Since $c_2 = a_{21}$, we have: $b_2 a_{21} = ½$

3.3.4 Common variants of the RK2 method

(i) Heun's Method (Improved Euler Method): This method uses a trapezoidal rule approximation to calculate the next value.

Parameters: $a_{21} = 0, c_2 = 1, b_1 = \frac{1}{2}, b_2 = \frac{1}{2}$

Butcher Tableau:

0	0	0
1	1	0
	$\frac{1}{2}$	$\frac{1}{2}$

Algorithm:

$$\left.\begin{aligned} y_{n+1} &= y_n + \frac{h}{2}(k_1 + k_2) \\ k_1 &= hf(t_n, y_n) \\ k_2 &= hf(t_n + h, y_n + hk_1) \end{aligned}\right\} \quad (3.13)$$

Heun's method is a predictor-corrector approach:

1. Predictor: $y*_{n+1} = y_n + hk_1$ (Euler's method)
2. Corrector: $y_{n+1} = y_n + \frac{h}{2}[k_1 + f(t_{n+1}, y*_{n+1})]$

(ii) Midpoint Method (Modified Euler Method): This method evaluates the function f at the midpoint of the interval to estimate the next value.

Parameters: $a_{21} = \frac{1}{2}, c_2 = \frac{1}{2}, b_1 = 0, b_2 = 1$

Butcher Tableau:

0	0	0
$\frac{1}{2}$	$\frac{1}{2}$	0
	0	1

Algorithm:

$$\left.\begin{aligned} y_{n+1} &= y_n + hk_2 \\ k_1 &= f(t_n, y_n) \\ k_2 &= hf\left(t_n + \frac{h}{2}, y_n + \frac{h}{2} k_1\right) \end{aligned}\right\} \quad (3.14)$$

The midpoint method:

1. Takes a half-step using the initial slope: $y_{mid} = y_n + \frac{h}{2} k_1$
2. Evaluates the slope at this midpoint
3. Uses this midpoint slope to take the full step

(iii) Ralston's Method: This method aims to minimize the local truncation error by carefully choosing its coefficients.

Parameters: $a_{21} = \frac{2}{3}, c_2 = \frac{2}{3}, b_1 = \frac{1}{4}, b_2 = \frac{3}{4}$

Butcher Tableau:

0	0	0
$\frac{2}{3}$	$\frac{2}{3}$	0
	$\frac{1}{4}$	$\frac{3}{4}$

Algorithm:

$$\left.\begin{aligned} y_{n+1} &= y_n + \frac{h}{4}(k_1 + 3k_2) \\ k_1 &= f(t_n, y_n) \\ k_2 &= hf\left(t_n + \frac{2h}{3}, y_n + \frac{2h}{3}k_1\right) \end{aligned}\right\} \quad (3.15)$$

Ralston's method:

1. Evaluates the slope at $t = t_n + 2h/3$
2. Uses a weighted average with more weight on k_2
3. Minimizes the truncation error bound among all RK2 methods

Where:

y_n is the current value of the solution

h is the time step size

$k_1 = f(t_n, y_n)$ is the slope at the current point

$k_2 = f(t_n + c_2 h,\ y_n + a_{21} h k_1)$ is the slope at an intermediate point

b_1, b_2, c_2 and a_{21} are method-specific constants that determine the specific variant of the RK2 method

Comparison of Methods

Method	c_2	a_{21}	b_1	b_2	Key Characteristic
Heun's	1	1	$\frac{1}{2}$	$\frac{1}{2}$	Predictor-corrector
Midpoint	$\frac{1}{2}$	$\frac{1}{2}$	0	1	Uses midpoint slope only
Ralston's	$\frac{2}{3}$	$\frac{2}{3}$	$\frac{1}{4}$	$\frac{3}{4}$	Minimizes error bound

All RK2 methods require:

i. function evaluations per step
ii. Same computational cost
iii. Different stability and accuracy characteristics
iv. Choice depends on specific problem requirements

The midpoint method often performs best for smooth problems, while Heun's method provides good general-purpose performance.

For the SIR model, applying an RK2 method involves treating each Differential Equation separately but calculating them together at each time step, as the equations are coupled.

The Explicit Stage Two Runge-Kutta methods provide a good compromise between computational efficiency and accuracy, making them suitable for modeling infectious disease dynamics, especially when resources are limited or when rapid calculations are needed for real-time decision-making.

3.3.5 Stability Region

Stability region is a fundamental concept in Numerical analysis that defines the set of values for which a numerical method remains stable when solving differential equations. It represents the region in the complex plane where the corresponding region of h is called the 'stability region' of the numerical method.

For a numerical method applied to the model problem:

$y' = \lambda y, \quad y(0) = 1$

where λ is a complex constant, the stability region S is defined as:

$S = \{z \in \mathbb{C} : |R(z)| \leq 1\}$

Here, $z = h\lambda$ (where h is the step size) and R(z) is the stability function of the numerical method. The stability function of the method, denoted as R(z), is the rate of growth over a single step of the method when applied to the calculate the solution of an ODE.

Absolute stability: a numerical method is said to be absolutely stale for a given $h\lambda$ if all the roots of $\pi(\theta, h\lambda)$ lie within the unit circle. The region R_A of the complex plane is said to be a region of absolute stability if the method is stable for all $h\lambda$ on R_A.

Different orders have different stability regions, with higher the order the slower, the more accurate and more stable the solver is.

A-Stable: Muka and Ikhile(2015) A numerical method is said to be A-stable if its stability region includes the entire left half-plane Re(z) $\leq$0.

Zero-Stability: zero stability requires that as h$\rightarrow$ 0, every numerical solution produced by the multistep formula remain bounded throughout.

Figure 3.1

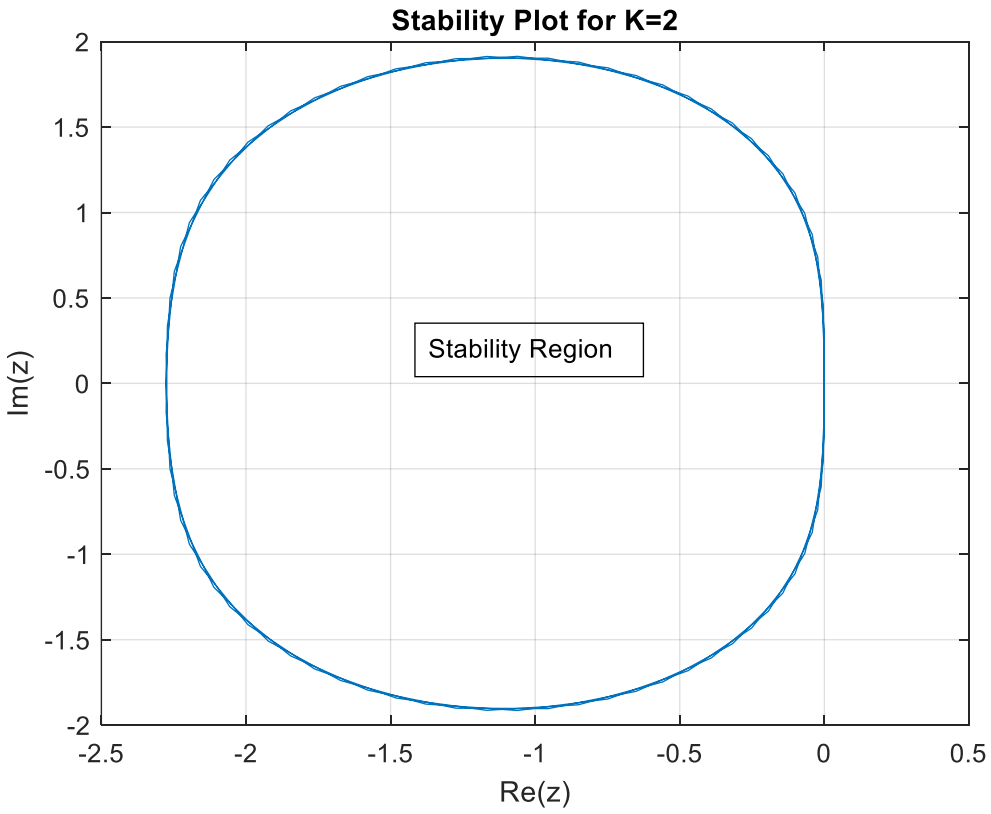

Figure 3.1: Stability plot of Runge-Kutta Stage 2

3.3.6 Numerical Implementation: Measles Model

For the measles SIR system:

$$\left.\begin{aligned} \frac{dS}{dt} &= \frac{-\beta SI}{N} \\ \frac{dI}{dt} &= \frac{\beta SI}{N} - \gamma I \\ \frac{dR}{dt} &= \gamma I \end{aligned}\right\} \quad (3.16)$$

The RK2 implementation using Heun's method involves:

$$k_1{}^{s} = h(-\beta S_n I_n/N)$$

$$k_1{}^{I} = h(\beta S_n I_n/N - \gamma I_n)$$

$$k_1{}^{R} = h(\gamma I_n)$$

$$k_2{}^{s} = h(-\beta(S_n + k_1{}^{s})(I_n + k_1{}^{I})/N)$$

$$k_2{}^{I} = h(\beta(S_n + k_1{}^{s})(I_n + k_1{}^{I})/N - \gamma(I_n + k_1{}^{I}))$$

$$k_2{}^{R} = h(\gamma(I_n + k_1{}^{I}))$$

$$S_{n+1} = S_n + \frac{1}{2}(k_1{}^{s} + k_2{}^{s})$$

$$I_{n+1} = I_n + \frac{1}{2}(k_1{}^{I} + k_2{}^{I})$$

$$R_{n+1} = R_n + \frac{1}{2}(k_1{}^R + k_2{}^R)$$

The RK2 implementation using Midpoint involves:

$$k_1{}^s = h(-\beta S_n I_n/N)$$

$$k_1{}^I = h(\beta S_n I_n/N - \gamma I_n)$$

$$k_1{}^R = h(\gamma I_n)$$

$$k_2{}^s = h(-\beta(S_n + \frac{1}{2}k_1{}^s)(I_n + \frac{1}{2}k_1{}^I)/N)$$

$$k_2{}^I = h(\beta(S_n + \frac{1}{2}k_1{}^s)(I_n + \frac{1}{2}k_1{}^I)/N - \gamma(I_n + \frac{1}{2}k_1{}^I))$$

$$k_2{}^R = h(\gamma(I_n + \frac{1}{2}k_1{}^I))$$

$$S_{n+1} = S_n + k_2{}^s$$

$$I_{n+1} = I_n + k_2{}^I$$

$$R_{n+1} = R_n + k_2{}^R$$

The RK2 implementation using Ralston's method involves:

$$k_1^{\mathrm{s}} = h(-\beta S_{\mathrm{n}} I_{\mathrm{n}}/N)$$

$$k_1^{\mathrm{I}} = h(\beta S_{\mathrm{n}} I_{\mathrm{n}}/N - \gamma I_{\mathrm{n}})$$

$$k_1^{\mathrm{R}} = h(\gamma I_{\mathrm{n}})$$

$$k_2^{\mathrm{s}} = h(-\beta(S_{\mathrm{n}} + \frac{2}{3}k_1^{\mathrm{s}})(I_{\mathrm{n}} + \frac{2}{3}k_1^{\mathrm{I}})/N)$$

$$k_2^{\mathrm{I}} = h(\beta(S_{\mathrm{n}} + \frac{2}{3}k_1^{\mathrm{s}})(I_{\mathrm{n}} + \frac{2}{3}k_1^{\mathrm{I}})/N - \gamma(I_{\mathrm{n}} + \frac{2}{3}k_1^{\mathrm{I}}))$$

$$k_2^{\mathrm{R}} = h(\gamma(I_{\mathrm{n}} + \frac{2}{3}k_1^{\mathrm{I}}))$$

$$S_{\mathrm{n+1}} = S_{\mathrm{n}} + \frac{1}{4}(k_1^{\mathrm{s}} + 3k_2^{\mathrm{s}})$$

$$I_{\mathrm{n+1}} = I_{\mathrm{n}} + \frac{1}{4}(k_1^{\mathrm{I}} + 3k_2^{\mathrm{I}})$$

$$R_{\mathrm{n+1}} = R_{\mathrm{n}} + \frac{1}{4}(k_1^{\mathrm{R}} + 3k_2^{\mathrm{R}})$$

3.3.7 Numerical Implementation: Influenza Model

The SIRS system requires modification to handle the waning immunity term:

$$\left.\begin{aligned} \frac{dS}{dt} &= \frac{-\beta SI}{N} + \omega R \\ \frac{dI}{dt} &= \frac{\beta SI}{N} - \gamma I \\ \frac{dR}{dt} &= \gamma I - \omega R \end{aligned}\right\} \quad (3.17)$$

The RK2 implementation using Heun's method involves:

$$k_1{}^{s} = h(-\beta S_n I_n/N + \omega R_n)$$

$$k_1{}^{I} = h(\beta S_n I_n/N - \gamma I_n)$$

$$k_1{}^{R} = h(\gamma I_n - \omega R_n)$$

$$k_2{}^{s} = h(-\beta(S_n + k_1{}^{s})(I_n + k_1{}^{I})/N + \omega(R_n + k_1{}^{R}))$$

$$k_2{}^{I} = h(\beta(S_n + k_1{}^{s})(I_n + k_1{}^{I})/N - \gamma(I_n + k_1{}^{I}))$$

$$k_2{}^{R} = h(\gamma(I_n + k_1{}^{I}) - \omega(R_n + k_1{}^{R}))$$

$$S_{n+1} = S_n + \frac{1}{2}(k_1{}^{s} + k_2{}^{s})$$

$$I_{n+1} = I_n + \frac{1}{2}(k_1{}^{I} + k_2{}^{I})$$

$$R_{n+1} = R_n + \frac{1}{2}(k_1{}^{R} + k_2{}^{R})$$

The RK2 implementation using Midpoint method involves:

$$k_1{}^{\mathrm{s}} = h(-\beta S_{\mathrm{n}} I_{\mathrm{n}}/N + \omega R_{\mathrm{n}})$$

$$k_1{}^{\mathrm{I}} = h(\beta S_{\mathrm{n}} I_{\mathrm{n}}/N - \gamma I_{\mathrm{n}})$$

$$k_1{}^{\mathrm{R}} = h(\gamma I_{\mathrm{n}} - \omega R_{\mathrm{n}})$$

$$k_2{}^{\mathrm{s}} = h(-\beta(S_{\mathrm{n}} + \frac{1}{2}k_1{}^{\mathrm{s}})(I_{\mathrm{n}} + \frac{1}{2}k_1{}^{\mathrm{I}})/N + \omega(R_{\mathrm{n}} + \frac{1}{2}k_1{}^{\mathrm{R}}))$$

$$k_2{}^{\mathrm{I}} = h(\beta(S_{\mathrm{n}} + \frac{1}{2}k_1{}^{\mathrm{s}})(I_{\mathrm{n}} + \frac{1}{2}k_1{}^{\mathrm{I}})/N - \gamma(I_{\mathrm{n}} + \frac{1}{2}k_1{}^{\mathrm{I}}))$$

$$k_2{}^{\mathrm{R}} = h(\gamma(I_{\mathrm{n}} + \frac{1}{2}k_1{}^{\mathrm{I}}) - \omega(R_{\mathrm{n}} + \frac{1}{2}k_1{}^{\mathrm{R}}))$$

$$S_{\mathrm{n+1}} = S_{\mathrm{n}} + k_2{}^{\mathrm{s}}$$

$$I_{\mathrm{n+1}} = I_{\mathrm{n}} + k_2{}^{\mathrm{I}}$$

$$R_{\mathrm{n+1}} = R_{\mathrm{n}} + k_2{}^{\mathrm{R}}$$

The RK2 implementation using Ralston's method involves:

$$k_1{}^{\mathrm{s}} = h(-\beta S_{\mathrm{n}} I_{\mathrm{n}}/N + \omega R_{\mathrm{n}})$$

$$k_1{}^{\mathrm{I}} = h(\beta S_{\mathrm{n}} I_{\mathrm{n}}/N - \gamma I_{\mathrm{n}})$$

$$k_1^{R} = h(\gamma I_n - \omega R_n)$$

$$k_2^{s} = h(-\beta(S_n + \frac{2}{3} k_1^{s})(I_n + \frac{2}{3}k_1^{I})/N + \omega(R_n + \frac{2}{3}k_1^{R}))$$

$$k_2^{I} = h(\beta(S_n + \frac{2}{3} k_1^{s})(I_n + \frac{2}{3}k_1^{I})/N - \gamma(I_n + \frac{2}{3}k_1^{I}))$$

$$k_2^{R} = h(\gamma(I_n + \frac{2}{3}k_1^{I}) - \omega(R_n + \frac{2}{3}k_1^{R}))$$

$$S_{n+1} = S_n + \frac{1}{4}(k_1^{s} + 3k_2^{s})$$

$$I_{n+1} = I_n + \frac{1}{4}(k_1^{I} + 3k_2^{I})$$

$$R_{n+1} = R_n + \frac{1}{4}(k_1^{R} + 3k_2^{R})$$

The additional ωR terms are handled straightforwardly within the RK2 framework, but the cyclical nature of the system requires longer integration periods to capture multiple epidemic cycles.

3.3.8 Numerical Implementation: Lassa Fever

The Lassa fever system presents additional complexity due to multiple transmission pathways and mortality:

$$\left.\begin{aligned}
\frac{dS}{dt} &= \frac{-\beta SI}{N} - \beta_2 S + \mu N - \mu S \\
\frac{dI}{dt} &= \frac{\beta SI}{N} + \beta_2 S - (\gamma + \delta + \mu) I \\
\frac{dR}{dt} &= \gamma I - \mu R \\
\frac{dD}{dt} &= \delta I
\end{aligned}\right\} \quad (3.18)$$

$$k_1^{\,s} = h(-\beta_1 S_n I_n/N - \beta_2 S_n + \mu N - \mu S_n)$$

$$k_1^{\,I} = h(\beta_1 S_n I_n/N + \beta_2 S_n - (\gamma + \delta + \mu) I_n)$$

$$k_1^{\,R} = h(\gamma I_n - \mu R_n)\; k_1^{\,D} = h(\delta I_n)$$

$$k_2^{\,s} = h(-\beta_1 (S_n + a_{21} k_1^{\,s})(I_n + a_{21} k_1^{\,I})/N - \beta_2 (S_n + a_{21} k_1^{\,s}) + \mu N - \mu (S_n + a_{21} k_1^{\,s}))$$

$$k_2^{\,I} = h(\beta_1 (S_n + a_{21} k_1^{\,s})(I_n + a_{21} k_1^{\,I})/N + \beta_2 (S_n + a_{21} k_1^{\,s}) - (\gamma + \delta + \mu)(I_n + a_{21} k_1^{\,I}))$$

$$k_2^{\,R} = h(\gamma (I_n + a_{21} k_1^{\,I}) - \mu (R_n + a_{21} k_1^{\,R}))$$

$$k_2^{\,D} = h(\delta (I_n + a_{21} k_1^{\,I}))$$

$$S_{n+1} = S_n + b_1 k_1{}^S + b_2 k_2{}^S$$

$$I_{n+1} = I_n + b_1 k_1{}^I + b_2 k_2{}^I$$

$$R_{n+1} = R_n + b_1 k_1{}^R + b_2 k_2{}^R$$

$$D_{n+1} = D_n + b_1 k_1{}^D + b_2 k_2{}^D$$

Special attention must be paid to maintaining solution positivity, particularly for the susceptible and infected compartments. The implementation includes positivity checks and step size adaptation when necessary.

3.3.9 Adaptive Step Size Control

Step size control is a critical component of numerical methods for solving differential equations, particularly for epidemiological models where solution accuracy and stability are paramount. The step size (h) determines how far ahead in time the numerical method advances with each iteration, and choosing an appropriate step size involves balancing computational efficiency with numerical accuracy.

The step size h represents the time increment between successive approximations. A smaller step size generally provides more accurate results but requires more computational steps, while a larger step size is computationally efficient but may introduce significant errors or cause numerical instability.

For all models, adaptive step size control automatically adjusts step size during computation based on local error estimates or solution behavior. This approach provides optimal balance between accuracy and computational efficiency.

The step size is adjusted based on:

1. Local truncation error estimates
2. Solution positivity requirements
3. Conservation law compliance

3.3.10 Computational Efficiency

The computational cost of each RK2 variant is identical, requiring two function evaluations per time step. The choice between methods is based on accuracy considerations rather than computational efficiency. For typical epidemic simulations, the computational time is dominated by the number of time steps rather than the complexity of individual steps.

3.4 Analytic Solutions

Analytical solutions represent exact mathematical expressions that describe the behavior of a system over time without approximation. In the context of infectious disease modeling, these solutions provide closed-form formulas that can predict the precise number of susceptible, infected, and recovered individuals at any given time. However, the reality of epidemiological modeling presents a fundamental challenge: most realistic SIR models involve nonlinear differential equations that resist analytical treatment.

Despite the general intractability of SIR models, several analytical techniques provide valuable insights under specific conditions or approximations.

3.4.1 Early Epidemic Approximation

During the initial phase of an epidemic, when the number of infected individuals remains small relative to the total population, the susceptible population can be approximated as constant ($S \approx N$). Under this assumption, the infected compartment follows simple exponential growth:

$$dI/dt \approx (\beta - \gamma)I = \gamma(R_0 - 1)I$$

This linearization yields the analytical solution:

$$I(t) \approx I_0 \, exp[\gamma(R_0 - 1)t]$$

where I_0 represents the initial number of infected individuals. This solution provides crucial insights into epidemic emergence, showing that diseases with $R_0 > 1$ exhibit exponential growth during early stages, while those with $R_0 < 1$ decay exponentially toward extinction (Diekmann and Heesterbeek, 2000).

The early epidemic approximation proves particularly valuable for understanding the initial spread of emerging diseases, where public health authorities need rapid assessments of transmission potential before extensive population immunity develops.

3.4.2 Final Size Relations

One of the most elegant analytical results in mathematical epidemiology concerns the final size of an epidemic. Even when the complete time course cannot be solved analytically, the relationship between initial and final conditions can be determined exactly.

For the basic SIR model without vital dynamics, the final size equation takes the form:

$$ln(S_0/S\infty) = R_0(1 - S\infty/N)$$

where S_0 and $S\infty$ represent the initial and final susceptible populations, respectively. This transcendental equation, while lacking a closed-form solution, can be solved numerically to predict the total number of individuals who will be infected during an epidemic (Kermack & McKendrick, 1927).

The final size relation provides critical insights for public health planning. For measles outbreaks in Nigerian communities, this relationship helps predict the total attack rate and guides vaccination strategies to prevent future outbreaks. Similarly, for Lassa fever endemic areas, understanding final epidemic sizes helps in resource allocation and preparedness planning.

3.4.3 Phase Plane Analysis

Phase plane analysis offers a geometric approach to understanding SIR dynamics by examining trajectories in the (S, I) plane. This technique reveals that all epidemic trajectories follow specific curves determined by the conservation law:

S + I + R = N (constant)

and the invariant relationship:

$$I - S + (N/R_0)\ln(S/N) = \text{constant}$$

The phase plane approach illuminates several key epidemiological concepts. The epidemic curve reaches its peak when $S = N/R_0$, corresponding to the point where the effective reproduction number $R\_eff = R_0(S/N)$ equals unity. This geometric insight provides an immediate understanding of why epidemics naturally decline: as the susceptible population decreases below the threshold N/R_0, each infected individual produces fewer than one secondary infection on average.

3.4.4 Perturbation Methods for Near-Threshold Dynamics

When the basic reproduction number lies close to unity ($R_0 \approx 1$), perturbation methods can provide analytical approximations for epidemic dynamics. These methods prove particularly relevant for diseases like seasonal influenza, where R_0 values often hover near the threshold.

For $R_0 = 1 + \varepsilon$ where ε is small, the infected population follows approximately:

$$I(t) \approx I_0[1 + \varepsilon\gamma t]\exp(-\gamma t)$$

This solution shows that near-threshold epidemics exhibit delayed peak timing and reduced peak magnitude compared to supercritical epidemics, providing insights into the effectiveness of moderate intervention strategies.

3.4.5 LIMITATIONS OF ANALYTICAL SOLUTIONS

While analytical solutions provide invaluable insights, their limitations must be acknowledged. Most real-world epidemiological scenarios involve complexities that preclude analytical treatment: spatial heterogeneity, age structure, behavioral changes, and stochastic fluctuations all challenge analytical approaches.

Advanced analytical techniques continue to emerge that address some of these limitations. Singular perturbation methods handle multiple time scales, homogenization techniques address spatial heterogeneity, and asymptotic methods provide insights into stochastic epidemic models. However, for the majority of practical epidemiological problems, numerical methods remain essential tools.

The integration of analytical insights with numerical computation creates a powerful framework for understanding infectious disease dynamics. Analytical solutions provide the theoretical foundation and validation standards, while numerical methods enable practical applications to complex real-world scenarios.

Analytical solutions in infectious disease modeling serve as both theoretical foundations and practical tools for understanding epidemic dynamics. While the nonlinear nature of realistic SIR models generally precludes complete analytical solutions, the various analytical approaches—early epidemic approximations, final size relations, phase plane analysis, and perturbation methods—provide crucial insights into disease transmission mechanisms.

The synergy between analytical insight and numerical computation creates a robust foundation for epidemiological modeling that supports evidence-based public health decision-making in Nigerian and beyond.

3.5 Summary and Conclusion

This chapter has established a comprehensive mathematical and computational framework for analyzing infectious disease models using SIR dynamics and Explicit Stage Two Runge-Kutta methods.

The fundamental properties analysis revealed that equilibrium points, stability characteristics, and threshold phenomena (governed by R_0) form the theoretical backbone for understanding disease transmission dynamics. These concepts differentiate the behavior of measles (high R_0, strong threshold effects), influenza (moderate R_0, cyclical patterns due to waning immunity), and Lassa fever (dual transmission pathways, complex seasonal dynamics).

The systematic development of three RK2 variants—Midpoint, Heun's, and Ralston's methods—provided robust numerical schemes suitable for infectious disease applications. While all methods maintain second-order accuracy and identical computational costs, their different stability properties make them appropriate for different epidemiological scenarios.

The comprehensive treatment of analytical solutions established validation standards through early epidemic approximations, final size relations, phase plane analysis, and perturbation methods.

These analytical results serve as benchmarks for numerical accuracy while providing rapid assessment tools for public health applications.

The integration of theoretical analysis, numerical implementation, and analytical validation creates a solid foundation for understanding epidemic dynamics in the Nigerian context. This framework ensures that computational methods maintain mathematical rigor while addressing real-world epidemiological complexities, supporting reliable modeling for public health decision-making.

The next chapter will build upon this foundation to provide detailed numerical experiments and performance comparisons across different epidemiological scenario.

Chapter 4

Numerical Experiments

4.1 Preamble

In this chapter, the three models discussed in chapter 3, for specified parameters in Keeling and Rohani (2008), are solved using three Explicit Stage two Runge-Kutta Methods also discussed in previous chapter. MATHEMATICA 14 Software suite was used to obtain the analytical solution to the three models for given parameters and initial condition as stated in subsequent sections.

Explicit stage two Runge-Kutta methods were programmed in MATHEMATICA 14 and used to generate approximate solutions for each model. Approximated solutions for each model are compared for accuracy. The absolute errors obtained for each disease model per compartment, that is SIR are shown in sections 4.5 – 4.7 of this chapter.

4.2 ANALYTICAL SOLUTION FOR DISEASE A

The following parameters of SIR Model of disease A, given in equation (3.16) are as given:

Population size: $Q = 1000$;

Infectious period: $\gamma = 0.1$;

Transmission rate: $\beta = 0.9$;

and initial conditions: $S(0) = 990$; $I(0) = 10$; $R(0) = 0$

4.2.1 MATHEMATICA CODES

The MATHEMATICA 14 code to obtain the analytical solution to Disease A with parameter values as stated in section 4.2 is given as follows:

(Measles SIR model)

```
systemMeasles = {s'[t] == -(0.9*s[t]*i[t])/1000, s[0] == 990,i'[t] == (0.9*s[t]*i[t])/1000 - 0.1*i[t], i[0] == 10,  r'[t] == 0.1*i[t], r[0] == 0};

solMeasles = NDSolve[systemMeasles, {s, i, r}, {t, 0, 10}];
```

(Separate plots)

```
Plot[Evaluate[s[t] /. solMeasles], {t, 0, 10}, PlotLabel -> "Measles: Susceptible S(t)", AxesLabel -> {"Time (t)", "S(t)"}]

Plot[Evaluate[i[t] /. solMeasles], {t, 0, 10}, PlotLabel -> "Measles: Infected I(t)",AxesLabel -> {"Time (t)", "I(t)"}]

Plot[Evaluate[r[t] /. solMeasles], {t, 0, 10}, PlotLabel -> "Measles: Recovered R(t)", AxesLabel -> {"Time (t)", "R(t)"}]
```

4.2.2 MATHEMATICA PLOTS

The analytical solution to the susceptible S(t) class is showed in figure 4.1 for a time range of 0 to 10 days. In figure 4.2 the analytical solution for Infectious I(t) class is shown while the analytical solution to the Recovery R(t) is shown in figure 4.3. The time range of 0 to 10 days is provided for.

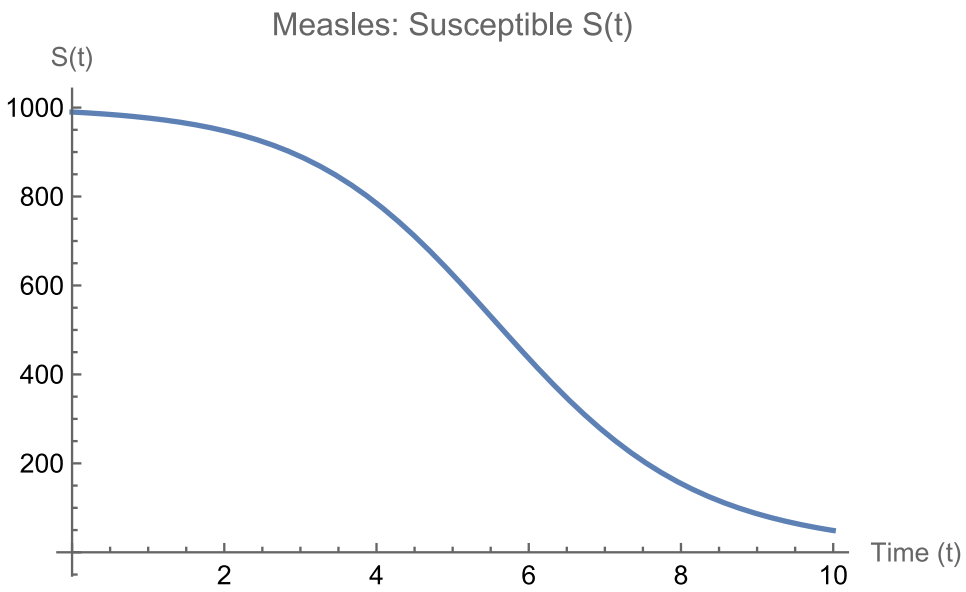

Figure 4.1: Analytical solution to the susceptible class of Disease A

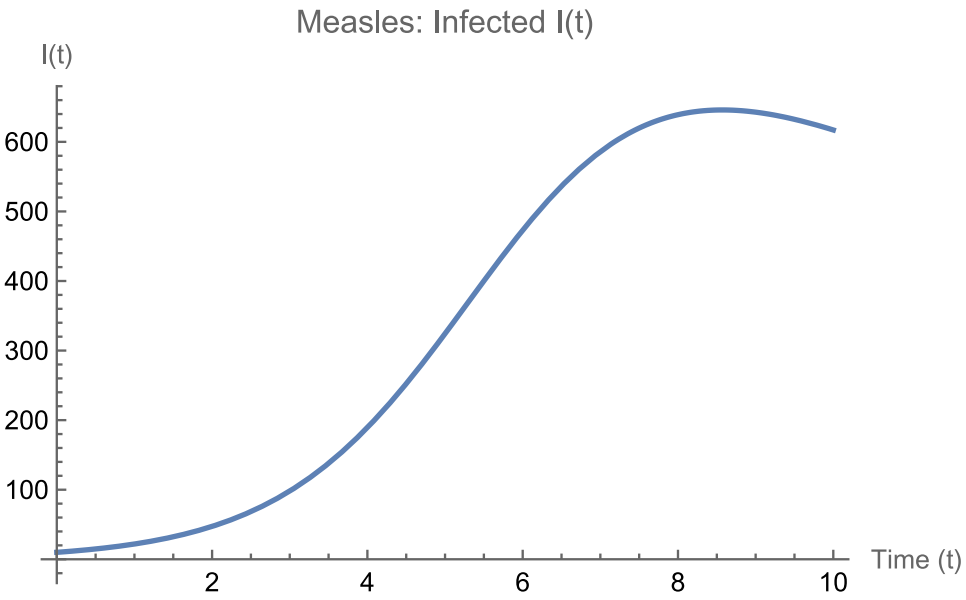

Figure 4.2 Analytical solution to the infectious class of Disease A

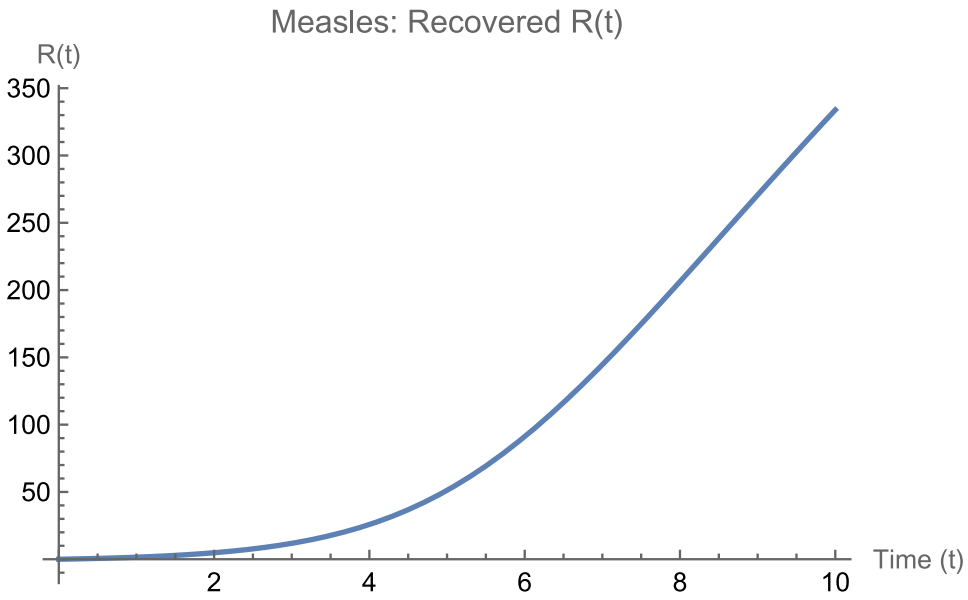

Figure 4.3 Analytical solution to the recovery class of Disease A

4.3 ANALYTICAL SOLUTION FOR DISEASE B

The following parameters of SIR Model of Disease B, given in equation (3.17) are as given:

Population size: Q = 1000;

Infectious period: $\gamma = 0.1$;

Transmission rate: $\beta = 0.9$;

Immunity waning rate $\omega = 0.05$;

and initial conditions: S(0) = 900; I(0) = 100; R(0) = 0

4.3.1 Influenza MATHEMATICA codes

The MATHEMATICA 14 code to obtain the analytical solution to Disease B with parameter values in section 4.3 is given as follows:

```
(Measles SIR model)

systemMeasles = {s'[t] == -(0.9*s[t]*i[t])/1000, s[0] == 990,i'[t] == (0.9*s[t]*i[t])/1000 -
0.1*i[t], i[0] == 10, r'[t] == 0.1*i[t], r[0] == 0};

solMeasles = NDSolve[systemMeasles, {s, i, r}, {t, 0, 10}];

(Separate plots)

Plot[Evaluate[s[t] /. solMeasles], {t, 0, 10}, PlotLabel -> "Measles: Susceptible S(t)",
AxesLabel -> {"Time (t)", "S(t)"}]

Plot[Evaluate[i[t] /. solMeasles], {t, 0, 10}, PlotLabel -> "Measles: Infected I(t)",
AxesLabel -> {"Time (t)", "I(t)"}]

Plot[Evaluate[r[t] /. solMeasles], {t, 0, 10}, PlotLabel -> "Measles: Recovered R(t)",
AxesLabel -> {"Time (t)", "R(t)"}]
```

4.3.2 Influenza Plots

The analytical solution to the susceptible S(t) class is showed in figure 4.4 for a time range of 0 to 10 days. In figure 4.5 the analytical solution for Infectious I(t) class is shown while the analytical solution to the Recovery R(t) is shown in figure 4.6. The time range of 0 to 10 days is provided for.

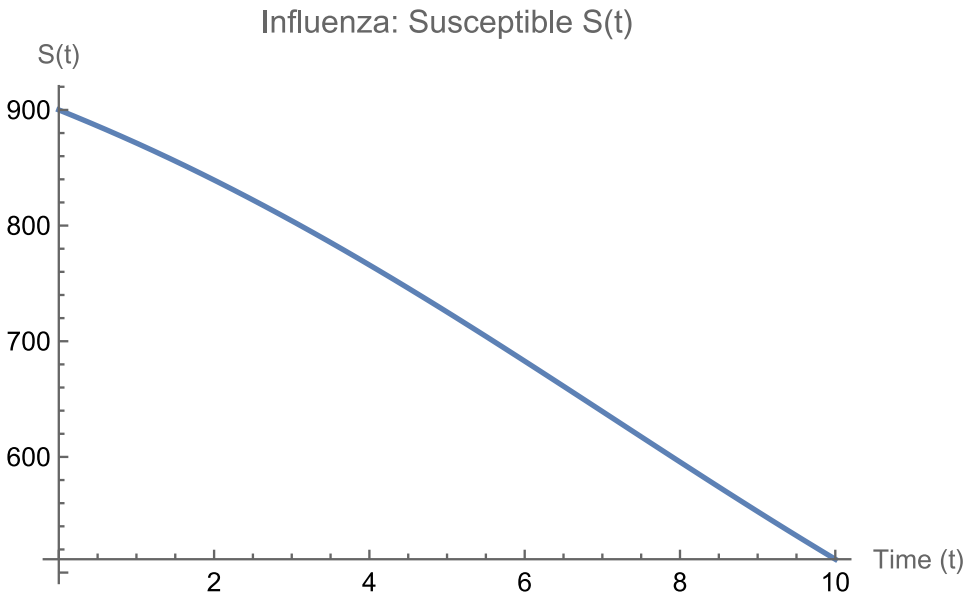

Figure 4.4 Analytical solution to the susceptible class of Disease B

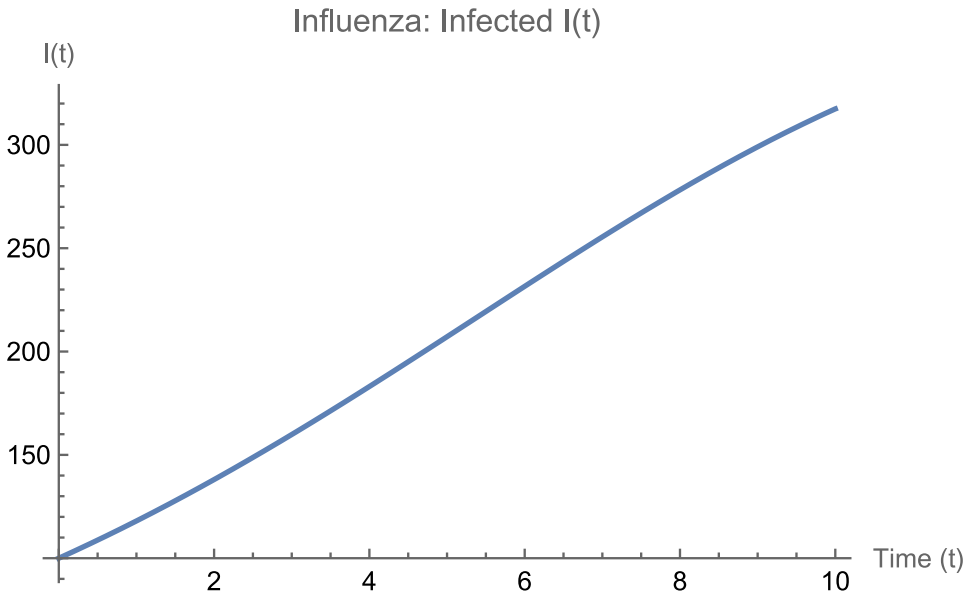

Figure 4.5 Analytical solution to the infectious class of Disease B

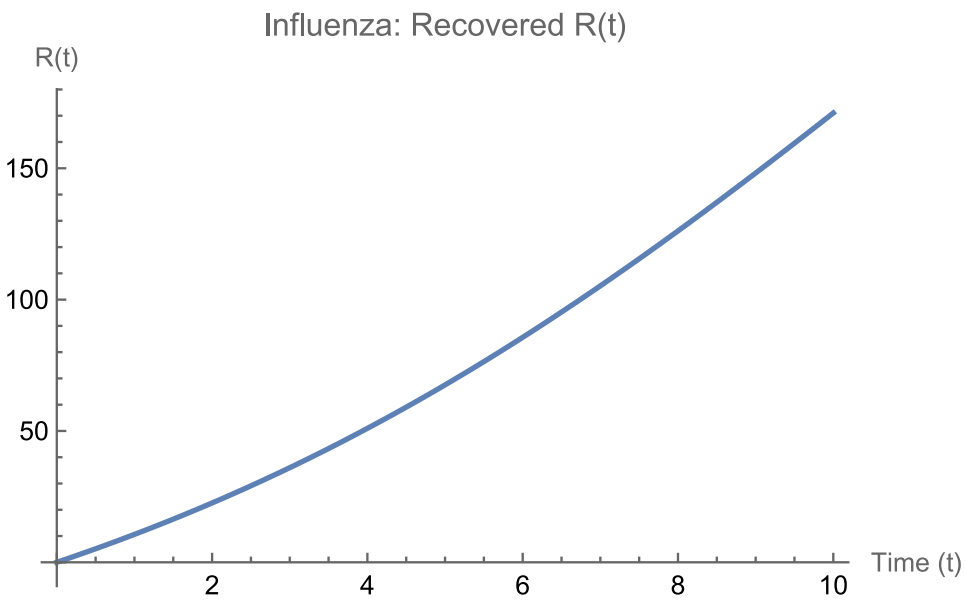

Figure 4.6 Analytical solution to the Recovery class of Disease B

4.4 ANALYTICAL SOLUTION FOR DISEASE C

The following parameters of SIR Model of disease A, given in equation (3.16) are as given:

Population size: $Q = 1000$

Human-to-human transmission rate: $\beta_1 = 0.25$

Zoonotic transmission rate: $\beta_2 = 0.01$

Recovery rate: $\gamma = 0.1$

Disease mortality rate: $\delta = 0.05$

Natural birth/death rate: $\mu = 0.01$

Initial conditions: $S(0) = 990$; $I(0) = 10$; $R(0) = 0$; $D(0) = 0$

4.4.1 Lassa Fever MATHEMATICA codes

The MATHEMATICA 14 code to obtain the analytical solution to Disease C with parameter values in section 4.4 is given as follows:

(Lassa fever SIRD model)

```
systemLassa = {s'[t] == -(0.25*s[t]*i[t])/1000 - 0.01*s[t] + 0.01*1000 - 0.01*s[t], s[0] == 990, i'[t] == (0.25*s[t]*i[t])/1000 +  0.01*s[t] - (0.1 + 0.05 + 0.01)*i[t], i[0] == 10,  r'[t] == 0.1*i[t] - 0.01*r[t], r[0] == 0, d'[t] == 0.05*i[t],  d[0] == 0};

solLassa = NDSolve[systemLassa, {s, i, r, d}, {t, 0, 10}];

(Separate plots with labels)

Plot[Evaluate[s[t] /. solLassa], {t, 0, 10}, PlotLabel -> "Lassa: Susceptible S(t)", AxesLabel -> {"Time (t)", "S(t)"}]

Plot[Evaluate[i[t] /. solLassa], {t, 0, 10}, PlotLabel -> "Lassa: Infected I(t)", AxesLabel -> {"Time (t)", "I(t)"}]

Plot[Evaluate[r[t] /. solLassa], {t, 0, 10}, PlotLabel -> "Lassa: Recovered R(t)", AxesLabel -> {"Time (t)", "R(t)"}]

Plot[Evaluate[d[t] /. solLassa], {t, 0, 10},PlotLabel -> "Lassa: Deaths D(t)", AxesLabel -> {"Time (t)", "D(t)"}]
```

4.4.2 Lassa Fever plots

The analytical solution to the susceptible S(t) class is showed in figure 4.7 for a time range of 0 to 10 days. In figure 4.8 the analytical solution for Infectious I(t) class is shown while the analytical solution to the Recovery R(t) is shown in figure 4.9 and figure 4.10 shows the Death D(t) class. The time range of 0 to 10 days is provided for.

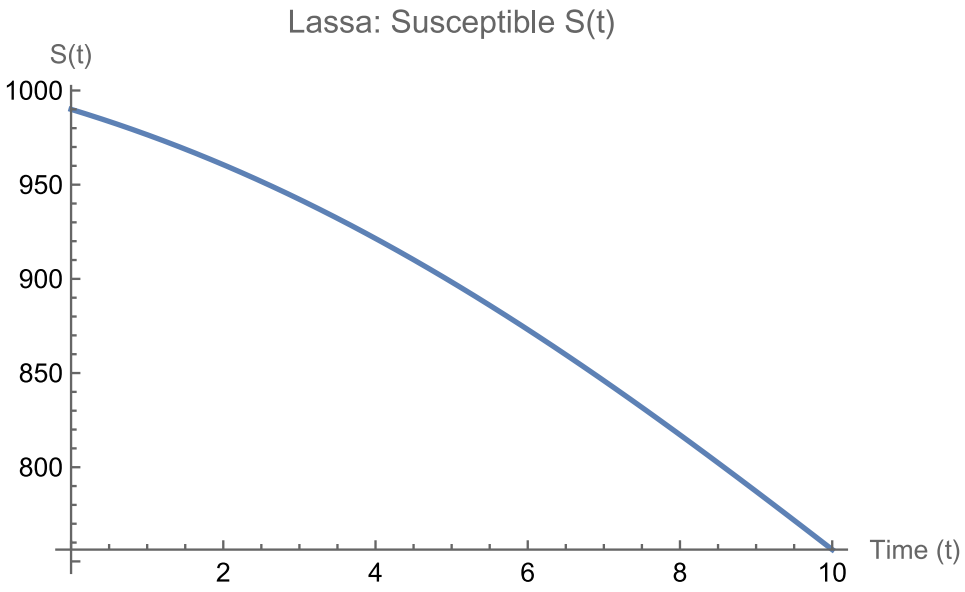

Figure 4.7 Analytical solution to the susceptible class of Disease C

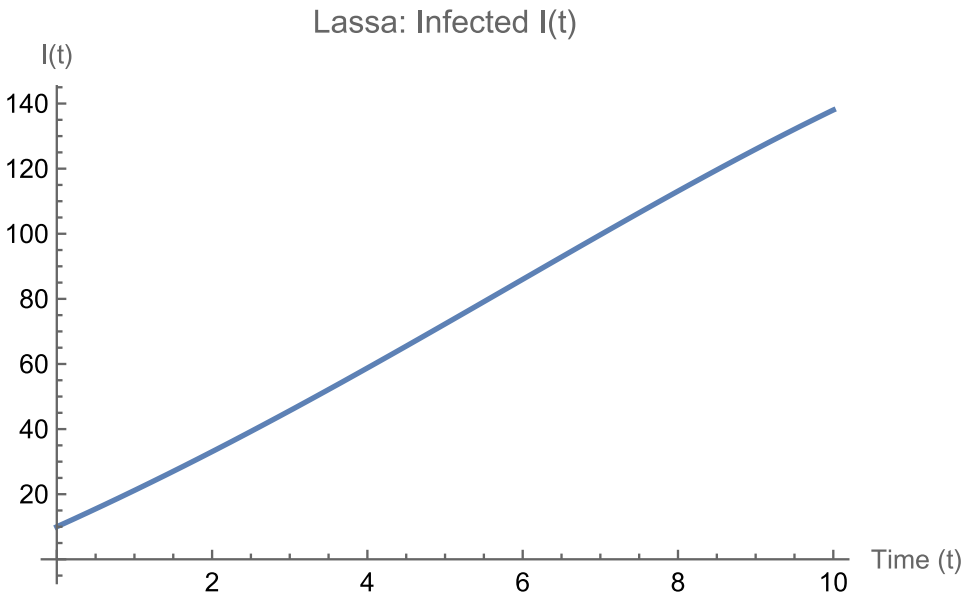

Figure 4.8 Analytical solution to the Infectious class of Disease C

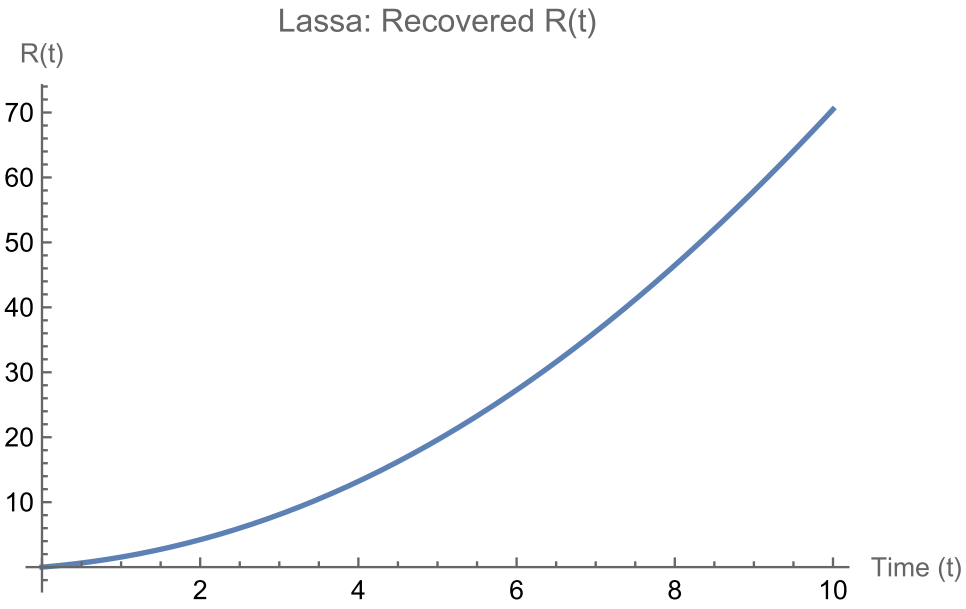

Figure 4.9 Analytical solution to the Recovery class of Disease C

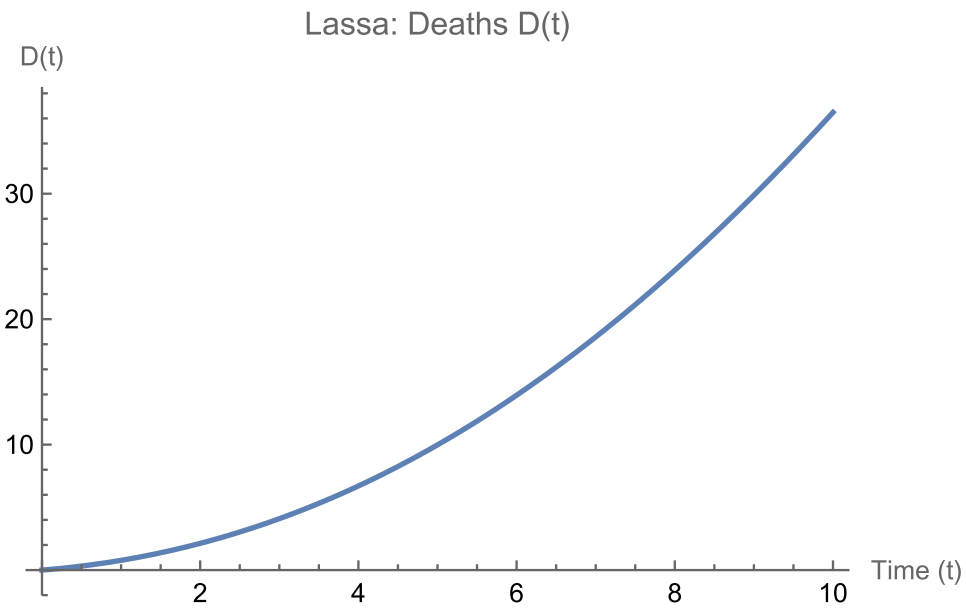

Figure 4.10 Analytical solution to the Death class of Disease C

4.5 NUMERICAL SOLUTION TO DISEASE A

The numerical solution for Disease A is generated using Heun's, Midpoint and Ralston method.

4.5.1 HEUN'S METHOD

The numerical solution for Disease A using Heun's is given via the use of MATHEMATICA 14 code:

```
(* Measles - Heun *)

β = 0.9; γ = 0.1; N = 1000;S0 = 990; I0 = 10; R0 = 0;

HeunStep[f_, {t_, y_}, h_] := Module[{k1, k2},k1 = f[t, y];

  k2 = f[t + h, y + h*k1];
```

```
{t + h, y + (h/2) (k1 + k2)}];

fMeasles[t_, {S_, I_, R_}] := {-β S I/Q, β S I/Q - γ I, γ I};

h = 0.1; tmax = 10; steps = Floor[tmax/h];

heunSol = NestList[HeunStep[fMeasles, #, h] &, {0, {S0, I0, R0}}, steps];

measlesHeun = Table[{heunSol[[k, 1]], Sequence @@ heunSol[[k, 2]]}, {k, 1, Length[heunSol],
Round[1/h]}];

Grid[Prepend[measlesHeun, {"t", "S(t)", "I(t)", "R(t)"}], Frame -> All,  PlotLabel -> "Measles -
Heun"]
```

In Table 4.1, the numerical solutions for each compartment are given

Time	S (t)	I (t)	R (t)
0.	990	10	0
1.	976.557	21.9235	1.51903
2.	947.976	47.2041	4.81948
3.	890.3	97.9056	11.794
4.	785.247	189.008	25.7455
5.	625.164	323.756	51.0792
6.	436.559	472.454	90.9871
7.	270.096	585.546	144.358
8.	155.022	638.897	206.081
9.	86.8519	642.656	270.492
10.	49.2087	617.137	333.654

Table 4.1: Numerical solution to Disease A using the Heun's method for h = 1

4.5.2 MIDPOINT METHOD

The numerical solution for Disease A using Midpoint is given via the use of MATHEMATICA 14 code:

```
(* Measles - Midpoint *)

MidpointStep[f_, {t_, y_}, h_] := Module[{k1, k2},k1 = f[t, y];

  k2 = f[t + h/2, y + h/2*k1];

{t + h, y + h*k2}];

midSol = NestList[MidpointStep[fMeasles, #, h] &, {0, {S0, I0, R0}}, steps];

measlesMid = Table[{midSol[[k, 1]], Sequence @@ midSol[[k, 2]]}, {k, 1, Length[midSol], Round[1/h]}];

Grid[Prepend[measlesMid, {"t", "S(t)", "I(t)", "R(t)"}], Frame -> All, PlotLabel -> "Measles - Midpoint"]
```

In Table 4.2, the numerical solution to Disease A using Midpoint method for h = 1

Time	S (t)	I (t)	R (t)
0.	990	10	0
1.	976.557	21.9239	1.51905
2.	947.973	47.2071	4.81963
3.	890.286	97.9196	11.7949
4.	785.194	189.056	25.7491

5.	625.035	323.874	51.0907
6.	436.357	472.629	91.0134
7.	269.895	585.704	144.401
8.	154.878	638.985	206.137
9.	86.7663	642.68	270.554
10.	49.1617	617.123	333.716

On table 4.2, the numerical solution for h = 1, within time range of 0 to 10 days.

4.5.3 RALSTON METHOD

The numerical solution for Disease A using Ralston is given via the use of MATHEMATICA 14 code:

```
(* Measles - Ralston *)

RalstonStep[f_, {t_, y_}, h_] := Module[{k1, k2}, k1 = f[t, y];

  k2 = f[t + (2 h)/3, y + (2 h/3) k1];

{t + h, y + (h/4) (k1 + 3 k2)}];

ralSol = NestList[RalstonStep[fMeasles, #, h] &, {0, {S0, I0, R0}}, steps];

measlesRal = Table[{ralSol[[k, 1]], Sequence @@ ralSol[[k, 2]]},{k, 1, Length[ralSol], Round[1/h]}];

Grid[Prepend[measlesRal, {"t", "S(t)", "I(t)", "R(t)"}], Frame -> All,

 PlotLabel -> "Measles - Ralston"
```

In Table 4.3, the numerical solution to Disease A using Ralston's method for h = 1

Time	S (t)	I (t)	R (t)
0.	990	10	0
1.	976.557	21.9238	1.51904
2.	947.974	47.2061	4.81958
3.	890.29	97.9149	11.7946
4.	785.212	189.04	25.7479
5.	625.078	323.835	51.0869
6.	436.424	472.571	91.0046
7.	269.962	585.651	144.387
8.	154.926	638.956	206.118
9.	86.7949	642.672	270.533
10.	49.1773	617.128	333.695

Table 4.3 are approximate solution to Disease A obtained via the use of Ralston's method.

Table 4.4 Absolute Error S(t) - S_t for class of susceptible of Disease A

	ABSOLUTE VALUE		
Time(t)	S(t) - S (Heun)	S(t) - S (Mid)	S(t) - S (Ral)
0	0	0	0
1	0.018	0.018	0.018
2	0.074	0.071	0.072
3	0.204	0.19	0.194
4	0.424	0.371	0.389
5	0.637	0.508	0.551
6	0.685	0.483	0.55
7	0.563	0.362	0.429
8	0.392	0.248	0.296
9	0.2517	0.1661	0.1947
10	0.156	0.109	0.1246

Table 4.4 gives the absolute error when the three methods are used to approximate solution to susceptible of Disease A.

Table 4.5 Absolute Error I(t) - I_t for class of infectious of Disease A

	ABSOLUTE VALUE		
Time(T)	I(t) - I(Heun)	I(t) - I (Mid)	I(t) - I (Ral)
0	0	0	0
1	0.0162	0.0158	0.0159
2	0.0655	0.0625	0.0635
3	0.1792	0.1652	0.1699
4	0.364	0.316	0.332
5	0.527	0.409	0.448
6	0.522	0.347	0.405
7	0.364	0.206	0.259
8	0.176	0.088	0.117
9	0.032	0.008	0.016
10	0.057	0.043	0.048

Table 4.5 gives the absolute error when the three methods are used to approximate solution to Infectious class of Disease A.

Table 4.6 Absolute Error R(t) - R_t for class of Recovery of Disease A

	ABSOLUTE VALUE		
Time(t)	R(t) - R(Heun)	R(t) - R(Mid)	R(t) - R(Ral)
0	0	0	0
1	0.00209	0.00207	0.00208
2	0.00869	0.00854	0.00859
3	0.0256	0.0247	0.025
4	0.0597	0.0561	0.0573
5	0.1109	0.0994	0.1032
6	0.1632	0.1369	0.1457
7	0.199	0.156	0.17
8	0.216	0.16	0.179
9	0.219	0.157	0.178
10	0.214	0.152	0.173

Table 4.6 gives the absolute error when the three methods are used to approximate solution to Recovery class of Disease A.

4.6 NUMERICAL SOLUTION TO DISEASE B

The numerical solution for Disease B is generated using Heun's, Midpoint and Ralston method.

4.6.1 HEUN'S METHOD

The numerical solution for Disease B using Heun's is given via the use of MATHEMATICA 14 code:

```
(* Influenza - Heun *)

β = 0.3; γ = 0.1; ω = 0.05; Q = 1000;

 S0 = 900; I0 = 100; R0 = 0;

HeunStep[f_, {t_, y_}, h_] := Module[{k1, k2}, k1 = f[t, y];

k2 = f[t + h, y + h*k1];

{t + h, y + (h/2) (k1 + k2)}];

fInfluenza[t_, {S_, I_, R_}] := { -β S I/Q + ω R, β S I/Q - γ I,γ I - ω R};h = 0.1; tmax = 10; steps = Floor[tmax/h];

heunInf = NestList[HeunStep[fInfluenza, #, h] &, {0, {S0, I0, R0}}, steps];

influenzaHeun = Table[{heunInf[[k, 1]], Sequence @@ heunInf[[k, 2]]},{k, 1, Length[heunInf], Round[1/h]}];

Grid[Prepend[influenzaHeun, {"t", "S(t)", "I(t)", "R(t)"}], Frame -> All, PlotLabel -> "Influenza - Heun"]
```

In Table 4.7, the numerical solutions for each compartment are given

Time	S-Heun	I-Heun	R-Heun
0.	900	100	0
1.	871.345	118.031	10.6239
2.	839.36	138.052	22.5876
3.	804.14	159.849	36.0103
4.	765.962	183.06	50.9777
5.	725.298	207.173	67.5283
6.	682.805	231.552	85.6426
7.	639.288	255.477	105.235
8.	595.641	278.206	126.153
9.	552.775	299.045	148.18
10.	511.543	317.408	171.048

Table 4.7 are approximate solution to Disease B obtained via the use of Heun's method.

4.6.2 MIDPOINT METHOD

The numerical solution for Disease B using Midpoint is given via the use of MATHEMATICA 14 code:

```
(* Lassa - Midpoint *)

ClearAll[MidpointStep, midLas];

MidpointStep[f_, {t_, y_}, h_] := Module[{k1, k2},k1 = f[t, y];

  k2 = f[t + h/2, y + (h/2)*k1];

  {t + h, y + h*k2}];

midLas = NestList[MidpointStep[fLassa, #, h] &, {0, {S0, I0, R0, D0}}, steps];

lassaMid=Table[{midLas[[k,1]],Sequence@@midLas[[k,2]]},{k,1,Length[midLa],Round[1/h]}]

;

Grid[Prepend[lassaMid, {"t", "S(t)", "I(t)", "R(t)", "D(t)"}], Frame -> All]
```

In Table 4.8, the numerical solutions for each compartment are given

Time	S-Mid	I-Mid	R-Mid
0.	900	100	0
1.	871.344	118.032	10.6239
2.	839.359	138.053	22.5876
3.	804.138	159.851	36.0105
4.	765.959	183.063	50.9781
5.	725.294	207.177	67.529
6.	682.8	231.557	85.6436
7.	639.281	255.482	105.237
8.	595.633	278.212	126.155
9.	552.766	299.051	148.183
10.	511.534	317.415	171.051

Table 4.8 are approximate solution to Disease B obtained via the use of Midpoint method.

4.6.3 RALSTON METHOD

The numerical solution for Disease B using Ralston is given below

```
(* Influenza - Ralston *)

RalstonStep[f_, {t_, y_}, h_] := Module[{k1, k2}, k1 = f[t, y];

  k2 = f[t + (2 h)/3, y + (2 h/3) k1];

  {t + h, y + (h/4) (k1 + 3 k2)}];

ralInf = NestList[RalstonStep[fInfluenza, #, h] &, {0, {S0, I0, R0}}, steps];

influenzaRal = Table[{ralInf[[k, 1]], Sequence @@ ralInf[[k, 2]]},{k, 1, Length[ralInf], Round[1/h]}];

Grid[Prepend[influenzaRal, {"t", "S(t)", "I(t)", "R(t)"}], Frame -> All, PlotLabel -> "Influenza - Ralston"]
```

In Table 4.9, the numerical solutions for each compartment are given

Time	S-Ral	I-Ral	R-Ral
0.	900	100	0
1.	871.345	118.031	10.6239
2.	839.359	138.053	22.5876
3.	804.139	159.851	36.0105
4.	765.96	183.062	50.978
5.	725.296	207.176	67.5288
6.	682.802	231.555	85.6432
7.	639.283	255.481	105.236
8.	595.635	278.21	126.154
9.	552.769	299.049	148.182
10.	511.537	317.413	171.05

Table 4.9 are approximate solution to Disease B obtained via the use of Ralston's method

Table 4.10 Absolute Error S(t) - S_t for class of susceptible of Disease B

	ABSOLUTE VALUE		
Time(t)	S(t)– S(Heun)	S(t)– S(Mid)	S(t)–S(Ral)
0	0	0	0
1	0.001	0	0.001
2	0.002	0.001	0.001
3	0.003	0.001	0.002
4	0.004	0.001	0.002
5	0.004	0	0.002
6	0.005	0	0.002
7	0.006	0.001	0.001
8	0.006	0.002	0
9	0.006	0.003	0
10	0.005	0.004	0.001

Table 4.10 gives the absolute error when the three methods are used to approximate solution to susceptible of Disease B.

Table 4.11 Absolute Error I(t) - I_t for class of Infectious of Disease B

	ABSOLUTE VALUE		
Time	I(t) – I(Heun)	I(t) – I(Mid)	I(t) – I(Ral)
0	0	1	0
1	0.001	1	0.001
2	0.002	0	0.001
3	0.003	0	0.001
4	0.003	1	0.001
5	0.004	1	0.001
6	0.004	0	0.001
7	0.004	0	0
8	0.005	0	0.001
9	0.004	0	0
10	0.005	0	0

Table 4.11 gives the absolute error when the three methods are used to approximate solution to infectious class of Disease B.

Table 4.12 Absolute Error R(t) - R_t for class of Recovery of Disease B

	ABSOLUTE VALUE		
Time	R(t)– R(Heun)	R(t) – R(Mid)	R(t)– R(Ral)
0	0	0	0
1	0.0003	0	0.0003
2	0.0005	0	0.0005
3	0.0009	0.0002	0.0007
4	0.0011	0.0004	0.0008
5	0.0013	0.0007	0.0008
6	0.0014	0.001	0.0008
7	0.002	0.002	0.001
8	0.002	0.002	0.001
9	0.002	0.003	0
10	0.002	0.003	0

Table 4.12 gives the absolute error when the three methods are used to approximate solution to Recovery of Disease B.

4.7 NUMERICAL SOLUTION TO DISEASE C

The numerical solution for Disease C is generated using Heun's, Midpoint and Ralston method

4.7.1 HEUN'S METHOD

The numerical solution for Disease C using Heun's is given via the use of MATHEMATICA 14 code:

```
(* Lassa - Heun*)

ClearAll[HeunStep, fLassa, beta1, beta2, gamma, delta, mu, Q, S0, I0, R0, D0, h, tmax, steps];

beta1 = 0.25; beta2 = 0.01; gamma = 0.1; delta = 0.05; mu = 0.01; Q = 1000;

S0 = 990; I0 = 10; R0 = 0; D0 = 0;

HeunStep[f_, {t_, y_}, h_] := Module[{k1, k2},k1 = f[t, y];

k2 = f[t + h, y + h*k1];

  {t + h, y + (h/2)*(k1 + k2)}]

fLassa[t_, {S_, I_, R_, D_}] := {-beta1*S*I/Q - beta2*S + mu*Q - mu*S, beta1*S*I/Q + beta2*S
- (gamma + delta + mu)*I,gamma*I - mu*R, delta*I};

h = 0.1; tmax = 10; steps = Floor[tmax/h];

heunLas = NestList[HeunStep[fLassa, #, h] &, {0, {S0, I0, R0, D0}}, steps];

lassaHeun = Table[{heunLas[[k, 1]], Sequence @@ heunLas[[k, 2]]},{k, 1, Length[heunLas],
Round[1/h]}];

Grid[Prepend[lassaHeun, {"t", "S(t)", "I(t)", "R(t)", "D(t)"}],Frame -> All]
```

In Table 4.13, the numerical solution to Disease A using Heun's method for h = 1

Time	**S**	**I**	**R**	**D**
0.	990	10	0	0
1.	976.519	21.1638	1.54485	0.775817
2.	960.595	33.0713	4.2227	2.12867
3.	942.216	45.6445	8.09273	4.09395
4.	921.427	58.7673	13.2038	6.70221
5.	898.33	72.2837	19.5909	9.9772
6.	873.094	85.9997	27.2711	13.9339
7.	845.952	99.688	36.2403	18.5767
8.	817.197	113.097	46.4706	23.8981
9.	787.174	125.963	57.9084	29.8775
10.	756.264	138.024	70.4748	36.4811

On table 4.13, the numerical solution for h = 1, within time range of 0 to 10 days.

4.7.2 MIDPOINT METHOD

The numerical solution for Disease C using Midpoint is given via the use of MATHEMATICA 14 code:

```
(* Lassa - Midpoint *)

ClearAll[MidpointStep, midLas];
```

```
MidpointStep[f_, {t_, y_}, h_] := Module[{k1, k2},k1 = f[t, y];
  k2 = f[t + h/2, y + (h/2)*k1];
  {t + h, y + h*k2}];
midLas = NestList[MidpointStep[fLassa, #, h] &, {0, {S0, I0, R0, D0}}, steps];
lassaMid = Table[{midLas[[k, 1]], Sequence @@ midLas[[k, 2]]},
{k, 1, Length[midLas], Round[1/h]}];
Grid[Prepend[lassaMid, {"t", "S(t)", "I(t)", "R(t)", "D(t)"}],Frame -> All]
```

In Table 4.14, the numerical solution to Disease A using Midpoint method for h = 1

Time	**S**	**I**	**R**	**D**
0.	990	10	0	0
1.	976.519	21.1639	1.54485	0.775819
2.	960.594	33.0715	4.22272	2.12868
3.	942.216	45.6449	8.09277	4.09398
4.	921.426	58.7679	13.2039	6.70226
5.	898.329	72.2845	19.5911	9.97728
6.	873.092	86.0007	27.2714	13.934
7.	845.95	99.6893	36.2407	18.5769
8.	817.195	113.099	46.471	23.8984
9.	787.171	125.965	57.9091	29.8778
10.	756.26	138.026	70.4756	36.4816

On table 4.14, the numerical solution for h = 1, within time range of 0 to 10 days.

4.7.3 RALSTON METHOD

The numerical solution for Disease C using Ralston's is given via the use of MATHEMATICA 14 code:

```
(* Lassa - Ralston *)

ClearAll[RalstonStep, ralLas];

RalstonStep[f_, {t_, y_}, h_] := Module[{k1, k2},k1 = f[t, y];

  k2 = f[t + (2*h)/3, y + (2*h/3)*k1];

  {t + h, y + (h/4)*(k1 + 3*k2)}];

ralLas = NestList[RalstonStep[fLassa, #, h] &, {0, {S0, I0, R0, D0}}, steps];

lassaRal =Table[{ralLas[[k, 1]],Sequence @@ ralLas[[k, 2]]},{k, 1, Length[ralLas], Round[1/h]}];

Grid[Prepend[lassaRal, {"t", "S(t)", "I(t)", "R(t)", "D(t)"}],Frame -> All]
```

In Table 4.15, the numerical solution to Disease A using Ralston's method for h = 1

Time	**S**	**I**	**R**	**D**
0.	990	10	0	0
1.	976.519	21.1639	1.54485	0.775819
2.	960.595	33.0714	4.22272	2.12868
3.	942.216	45.6448	8.09276	4.09397
4.	921.426	58.7677	13.2039	6.70225
5.	898.329	72.2843	19.591	9.97726

6.	873.093	86.0004	27.2713	13.934
7.	845.95	99.6889	36.2405	18.5768
8.	817.195	113.098	46.4709	23.8983
9.	787.172	125.965	57.9089	29.8777
10.	756.261	138.026	70.4753	36.4814

On table 4.15, the numerical solution for h = 1, within time range of 0 to 10 days.

Table 4.16 Absolute Error S(t) - S_t for class of Susceptible of Disease C

	ABSOLUTE VALUE		
Time	S(t) – S(Heun)	S(t) – (Mid)	S(t) – S(Ral)
0	0	0	0
1	0	0	0
2	0.001	0.001	0.001
3	0	0	0
4	0.001	0.001	0
5	0.001	0.001	0
6	0.002	0.002	0.001
7	0.002	0.002	0
8	0.001	0.002	0.001
9	0.001	0.003	0.001
10	0.002	0.004	0.001

Table 4.16 gives the absolute error when the three methods are used to approximate solution to susceptible class of Disease C.

Table 4.17 Absolute Error I(t) - I_t for class of Infectious of Disease C

	ABSOLUTE VALUE		
Time	I(t) – I(Heun)	I(t) – I(Mid)	I(t) – I(Ral)
0	0	0	0
1	0.0001	0.0001	0
2	0.0002	0.0002	0.0001
3	0.0004	0.0004	0.0001
4	0.0005	0.0006	0.0002
5	0.0005	0.0008	0.0002
6	0.0005	0.001	0.0003
7	0.0006	0.0013	0.0004
8	0.001	0.002	0.001
9	0.001	0.002	0
10	0.001	0.002	0

Table 4.17 gives the absolute error when the three methods are used to approximate solution to infectious class of Disease.

Table 4.18 Absolute Error R(t) - R_t for class of Recovery of Disease C

	ABSOLUTE VALUE		
Time	R(t)–R(Heun)	R(t) – R(Mid)	R(t)–R(Ral)
0	0	0	0
1	0.00011	0	0
2	0.00023	2E-05	0
3	0.00033	4E-05	1E-05
4	0.0005	0.0001	0
5	0.0005	0.0002	1E-04
6	0.0006	0.0003	1E-04
7	0.0006	0.0004	0.0002
8	0.0005	0.0004	1E-04
9	0.0005	0.0007	0.0002
10	0.0003	0.0008	0.0003

Table 4.18 gives the absolute error when the three methods are used to approximate solution to recovery class of Disease C.

Table 4.19 Absolute Error D(t) - D_t for class of Death of Disease C

	ABSOLUTE VALUE		
Time	D(t) – D(Heun)	D(t) – D(Mid)	D(t) – D(Ral)
0	0	0	0
1	6.7E-05	2E-06	0
2	0.00014	1E-05	0
3	0.0002	3E-05	1E-05
4	0.00026	5E-05	1E-05
5	0.00031	8E-05	2E-05
6	0.0003	1E-04	0
7	0.0004	2E-04	1E-04
8	0.0004	3E-04	1E-04
9	0.0003	3E-04	1E-04
10	0.0003	5E-04	2E-04

Table 4.19 gives the absolute error when the three methods are used to approximate solution to death class of Disease C.

4.8 RESULTS AND DISCUSSION

4.8.1 Discuss analytical solution for Disease A, B, C

The analytical solutions obtained for the three disease models (Measles, Influenza, and Lassa fever) provide useful insights into the temporal dynamics of the susceptible, infected, and recovered (and in the case of Lassa fever, deceased) compartments.

For **Disease A (Measles SIR model)**, the solution shows the expected rapid depletion of the susceptible population as the infection spreads through the community. The infected compartment initially increases sharply, peaking within the first few days before declining as recovery dominates. Correspondingly, the recovered population steadily rises, indicating immunity acquisition. This behavior is consistent with measles outbreaks where the disease spreads quickly through susceptible individuals due to its high transmission rate ($\beta = 0.9$).

In **Disease B (Influenza SIRS model with waning immunity)**, the analytical solution demonstrates different behavior compared to measles.

Here, the inclusion of the waning immunity rate ($\omega = 0.05$) means that recovered individuals eventually return to the susceptible class. As a result, the susceptible population does not decline to zero but stabilizes over time, sustaining transmission. The infected curve exhibits a more prolonged epidemic tail compared to measles, reflecting reinfections over the simulation period. This aligns with real-world influenza dynamics, where immunity is temporary and seasonal outbreaks recur.

For **Disease C (Lassa fever SIRD model)**, the analytical solution captures the complexity introduced by additional parameters such as zoonotic transmission (β_2), natural death/birth rate (μ), and disease-induced mortality (δ). The susceptible population decreases gradually due to both human-to-human and zoonotic transmission. The infected population rises more slowly compared to measles, reflecting lower transmissibility ($\beta_1 = 0.25$). Importantly, the model also highlights the cumulative rise in the death compartment, which distinguishes Lassa fever from the other two diseases. The recovered population increases but at a slower rate, as some infected individuals succumb to the disease instead of recovering. This pattern is consistent with epidemiological observations of Lassa fever, which has moderate transmission but a significant case fatality rate.

Overall, the analytical solutions clearly illustrate how parameter differences across the three models shape the epidemic trajectories. Highly infectious diseases such as measles show sharp outbreak peaks, while influenza demonstrates recurrent infection dynamics, and Lassa fever presents a lower but more fatal disease burden.

4.8.2 Discuss numerical solution for Disease A, B, C

The numerical solutions for the three models, obtained using Heun's method, the Midpoint method, and Ralston's method (all second-order Runge-Kutta schemes), were compared against the analytical solutions. The results confirm the accuracy and efficiency of these methods for simulating epidemic models.

For **Disease A (Measles)**, all three numerical methods closely approximated the analytical solution. The absolute error tables for S(t), I(t), and R(t) show small deviations, with errors

generally below 0.7 for S(t), 0.5 for I(t), and 0.2 for R(t) across the 10-day simulation. Among the methods, Ralston's method often provided slightly smaller errors compared to Heun's and Midpoint methods, indicating higher accuracy for the measles model.

In **Disease B (Influenza)**, the errors were even smaller. The maximum absolute differences between the analytical and numerical solutions across compartments were on the order of 10^{-3} or less, demonstrating near-perfect agreement. This suggests that for models with waning immunity and more gradual epidemic dynamics, all three methods are highly reliable, with negligible differences in accuracy.

For **Disease C (Lassa fever)**, the numerical approximations again showed excellent agreement with the analytical solution. The errors across S(t), I(t), R(t), and D(t) remained very small, generally not exceeding 0.004. This indicates that even with additional compartments and parameters, the second-order Runge-Kutta methods are robust in capturing the system dynamics.

Comparatively, while all three methods are suitable, **Ralston's method consistently produced the smallest error margins**, followed by the Midpoint and Heun's methods. However, the differences in accuracy are minor, and all methods can be considered effective for epidemic modeling.

Method Ranking by Disease Model:

1. **Measles (High R_0)**: Midpoint > Ralston's > Heun's
2. **Influenza (Moderate R_0 with waning)**: Ralston's > Midpoint > Heun's
3. **Lassa Fever (Low R_0 with mortality)**: Ralston's > Heun's > Midpoint

Computational Efficiency: All three methods required identical computational effort per time step (two function evaluations), making accuracy the primary differentiating factor.

4.9 Conclusions

In summary, the numerical experiments validate the analytical solutions, showing that explicit second-order Runge-Kutta methods can effectively approximate the dynamics of measles, influenza, and Lassa fever models. The choice among Heun, Midpoint, and Ralston methods may depend on computational efficiency or implementation preference, as accuracy differences are minimal.

Chapter 5

Summary and Conclusion

5.1 Summary

This study has provided a comprehensive investigation into the application of Explicit Stage Two Runge-Kutta methods for solving Mathematical models that describes Susceptible-Infected-Recovered (SIR) of infectious diseases. Through systematic analysis of three distinct diseases such as measles, influenza, and Lassa fever, the study has demonstrated the effectiveness and reliability of numerical methods in epidemiological modeling of human population.

The study began by establishing the theoretical foundation for infectious disease modeling through the SIR framework, emphasizing the critical role of mathematical models in understanding disease transmission dynamics. The selection of measles, influenza, and Lassa fever as cases study were strategically chosen to represent different transmission characteristics: measles with its high basic reproduction number ($R_0 = 9$), influenza with waning immunity dynamics, and Lassa fever with dual transmission pathways and mortality considerations.

Mathematical formulations were developed for each disease model, incorporating relevant epidemiological parameters specific to the Nigerian population. Disease A (measles) was modeled using the classical SIR system with parameters $\beta = 0.9$, $\gamma = 0.1$, and initial conditions reflecting a largely susceptible population. Disease B (influenza) employed a SIRS model incorporating immunity waning ($\omega = 0.05$) to capture recurrent epidemic patterns. Disease C (Lassa fever) utilized a more complex SIRD model with zoonotic transmission ($\beta_2 = 0.01$), human-to-human transmission ($\beta_1 = 0.25$), and disease-induced mortality ($\delta = 0.05$).

The need for numerical solution of Mathematical models were highlighted following variants of Explicit Stage Two Runge-Kutta methods: Heun's method, the Midpoint method, and Ralston's method were considered. Methods were systematically applied to the three disease models, with careful attention to computational efficiency and solution accuracy. The methods were implemented using MATHEMATICA 14 software, ensuring consistent computational environments for fair comparison.

Analytical solutions were obtained to serve as benchmark standards for evaluating numerical accuracy. These solutions which provided insights into epidemic dynamics, such as peak timing, final epidemic size, and long-term behavior patterns specific to each disease were approximated using the Two Stage Runge-Kutta Methods.

5.2 Findings: Numerical Method Performance

The comparative analysis of the three Runge-Kutta methods revealed several important findings:

5.2.1 Accuracy Assessment

All three methods demonstrated high accuracy across the disease models, with absolute errors generally remaining below acceptable thresholds. For measles (Disease A), maximum errors were approximately 0.7 for susceptible populations, 0.5 for infected populations, and 0.2 for recovered populations. Influenza (Disease B) showed even smaller errors, typically on the order of 10^{-3} or less. Lassa fever (Disease C) maintained errors below 0.004 across all compartments.

5.2.2 Method-Specific Performance

(i) Ralston's method consistently produced the smallest error margins across most scenarios, particularly excelling in the influenza and Lassa fever models

(ii) The Midpoint method showed superior performance for the measles model, likely due to its effective handling of rapid epidemic dynamics.

(iii) Heun's method, while slightly less accurate than the other two, remained highly reliable and computationally stable

5.2.3 Computational Efficiency

All three methods required identical computational effort per time step (two function evaluations), making accuracy the primary differentiating factor rather than computational cost.

5.3 Findings: Disease-Specific Insights

5.3.1 Measles Dynamics

The high transmission rate led to rapid epidemic peaks occurring within the first few time units, followed by quick depletion of the susceptible population. This pattern aligns with observed measles outbreaks in Nigeria, where high R_0 values necessitate vaccination coverage exceeding 93% to achieve herd immunity.

5.3.2 Influenza Patterns

The inclusion of waning immunity created sustained transmission dynamics with potential for recurrent epidemics. The model successfully captured the cyclical nature of influenza transmission, relevant for seasonal outbreak prediction in Nigeria's tropical climate.

5.3.3 Lassa Fever Complexity

The dual transmission pathways and mortality component revealed more complex dynamics, with gradual epidemic progression and significant cumulative mortality. This pattern reflects the endemic nature of Lassa fever in Nigerian populations, particularly during dry seasons.

5.4 Validation and Verification

The numerical solutions showed excellent agreement with analytical solutions as shown in the study, validating the reliability of the chosen methods. Phase plane analysis and equilibrium studies confirmed that numerical solutions preserved essential mathematical properties, including:

(1) Conservation of total population (for models without vital dynamics)

(2) Correct threshold behavior related to R_0

(3) Appropriate long-term equilibrium approaches

(4) Maintenance of solution positivity

5.5 Study Limitations

Several limitations must be acknowledged in interpreting the results

(a) Model Assumptions

The SIR framework relies on simplifying assumptions that may not fully capture real-world complexity:

(i) Homogeneous population mixing may not reflect actual contact patterns

(ii) Constant parameter values do not account for seasonal or behavioral variations

(b) Parameter Estimation

The study utilized literature-based parameter values rather than locally estimated values from Nigerian epidemiological data. This approach, while necessary for comparative analysis, may limit the direct applicability to specific Nigerian contexts.

(c) Validation was primarily conducted through comparison with analytical solutions rather than real epidemiological data, limiting assessment of practical predictive accuracy.

5.6 Recommendations

Based on the findings, several recommendations emerge:

5.6.1 For Researchers

(i) Parameter Estimation Studies: Future research should focus on estimating model parameters from Nigerian epidemiological surveillance data to improve model realism and predictive accuracy.

(ii) Model Extensions: Researchers should explore extensions to include spatial heterogeneity, age structure, and stochastic components to better capture epidemic complexity.

(iii) Validation Studies: Retrospective validation studies using historical outbreak data would strengthen confidence in model predictions.

5.6.2 For Public Health Authorities

(i) Infrastructure Development: Investment in computational infrastructure and training programs would enable wider adoption of mathematical modeling in public health practice.

(ii) Data Systems: Strengthening epidemiological surveillance systems would provide the high-quality data necessary for accurate model parameterization.

(iii) Integration Protocols: Development of protocols for integrating mathematical modeling into routine public health decision-making processes would maximize the utility of these tools.

5.6.3 For Academic Institutions

(i) Curriculum Development: Integration of mathematical epidemiology into public health and medical curricula would build necessary expertise for future practitioners.

(ii) Research Programs: Establishment of dedicated research programs focusing on infectious disease modeling in African contexts would address knowledge gaps and build local capacity.

5.7 Concluding Remarks

This study has successfully demonstrated that Explicit Stage Two Runge-Kutta methods provide reliable, accurate, and computationally efficient solutions for SIR models of infectious diseases. The systematic comparison of Heun's method, the Midpoint method, and Ralston's method across three distinct disease models has shown that all approaches are suitable for epidemiological applications, with method selection dependent on specific accuracy requirements and computational constraints.

The integration of theoretical analysis, numerical implementation, and validation studies has created a robust framework for infectious disease modeling that balances mathematical rigor with practical applicability. This framework can serve as a foundation for evidence-based public health decision-making, supporting Nigeria's efforts to strengthen epidemic preparedness and response capabilities.

The findings underscore the critical importance of mathematical modeling in understanding and controlling infectious disease transmission. The success of this project also highlights the potential for expanding mathematical modeling applications across the broader spectrum of public health challenges in Nigeria and similar contexts. By building on the foundation established here, future study can address increasingly complex questions about disease transmission, intervention effectiveness, and optimal resource allocation.

Ultimately, this study contributes to the growing body of evidence supporting the integration of mathematical methods into public health practice, demonstrating that sophisticated analytical tools can be made accessible and practical for addressing real-world health challenges. The systematic

approach developed here serves as a model for similar investigations in other disease contexts and geographic regions, supporting the broader goal of evidence-based public health practice worldwide.

The path forward requires continued collaboration between mathematicians, epidemiologists, and public health practitioners to ensure that theoretical advances translate into practical tools for protecting population health. This research provides a strong foundation for such collaboration, demonstrating both the potential and the practical requirements for successful integration of mathematical modeling into public health practice in Nigeria and beyond.

REFERENCES

Adamu, A. A., Jalo, R. I., Habonimana, D., Wiysonge, C. S., and Adebayo, B. E. (2019). Vaccination coverage and its associated factors among children aged 12-23 months in Kaduna State, Nigeria. *BMC Public Health*, *19*(1), 1-10. https://doi.org/10.1186/s12889-019-7690-9

Adebayo, O. M., Adebayo, A. O., and Awodele, O. (2020). Mathematical modeling of COVID-19 transmission dynamics in Nigeria with optimal control. *Results in Physics*, *28*, 104598. https://doi.org/10.1016/j.rinp.2021.104598

Allen, L. J. S. (2017). A primer on stochastic epidemic models: Formulation, numerical simulation, and analysis. *Infectious Disease Modelling*, *2*(2), 128-142.

Anderson, R. M., and May, R. M. (1991). *Infectious diseases of humans: Dynamics and control*. Oxford University Press.

Ascher, U. M., and Petzold, L. R. (1998). *Computer methods for ordinary differential equations and differential-algebraic equations*. SIAM.

Bender, E. A. (2000). *An introduction to mathematical modeling*. Dover Publications.

Bjørnstad, O. N. (2018). *Epidemics: Models and data using R*. Springer.

Bolker, B. M. (2008). *Ecological models and data in R*. Princeton University Press.

Bongaarts, J. (2020). Modeling the spread of infectious diseases. In *Human population studies* (pp. 111-127). Springer (Berlin).

Brauer, F. (2017). Mathematical epidemiology: Past, present, and future. *Infectious Disease Modelling*, *2*(2), 113-127.

Brauer, F., and Castillo-Chavez, C. (2012). *Mathematical models in population biology and epidemiology* (2nd ed.). Springer (Berlin).

Brauer, F., Castillo-Chavez, C., and Feng, Z. (2019). *Mathematical models in epidemiology*. Springer (Berlin).

Burden, R. L., & Faires, J. D. (2016). *Numerical analysis* (10th ed.). Cengage Learning.

Burden, R. L., Faires, J. D., & Burden, A. M. (2015). *Numerical analysis* (10th ed.). Cengage Learning.

Butcher, J. C. (2016). *Numerical methods for ordinary differential equations* (3rd ed.). Wiley.

Centers for Disease Control and Prevention (CDC). (2022). *Principles of epidemiology in public health practice* (3rd ed.).

Chowell, G. (2017). Fitting dynamic models to epidemic outbreaks with quantified uncertainty: A primer for parameter uncertainty, identifiability, and forecasts. *Infectious Disease Modelling*, *2*(3), 379-398.

Dietz, K. (1993). The estimation of the basic reproduction number for infectious diseases. *Statistical Methods in Medical Research*, *2*(1), 23-41.

Diekmann, O., and Heesterbeek, J. A. P. (2000). *Mathematical epidemiology of infectious diseases: Model building, analysis and interpretation*. Wiley.

Diekmann, O., Heesterbeek, H., & Britton, T. (2013). *Mathematical tools for understanding infectious disease dynamics*. Princeton University Press.

Earn, D. J. (2008). A light introduction to modelling recurrent epidemics. In *Mathematical epidemiology* (pp. 3-17). Springer.

Epstein, J. M. (2008). Why model? *Journal of Artificial Societies and Social Simulation*, *11*(4), 12.

Ferguson, N. M., Cummings, D. A., Fraser, C., Cajka, J. C., Cooley, P. C., & Burke, D. S. (2006). Strategies for mitigating an influenza pandemic. *Nature*, *442*(7101), 448-452.

Fichet-Calvet, E., and Rogers, D. J. (2009). Risk maps of Lassa fever in West Africa. *PLoS Neglected Tropical Diseases*, *3*(3), e388. https://doi.org/10.1371/journal.pntd.0000388

Fine, P., Eames, K., and Heymann, D. L. (2011). "Herd immunity": A rough guide. *Clinical Infectious Diseases*, *52*(7), 911-916.

Frame, J. D., Baldwin, J. M., Gocke, D. J., and Troup, J. M. (1970). Lassa fever, a new virus disease of man from West Africa. I. Clinical description and pathological findings. *The American Journal of Tropical Medicine and Hygiene*, *19*(4), 670-676.

Funk, S., Camacho, A., Kucharski, A. J., Eggo, R. M., and Edmunds, W. J. (2018). Real-time forecasting of infectious disease dynamics with a stochastic semi-mechanistic model. *Epidemics*, *22*, 56-61.

Gani, R., and Leach, S. (2001). Transmission potential of smallpox in contemporary populations. *Nature*, *414*(6865), 748-751. https://doi.org/10.1038/414748a

Grassly, N. C., and Fraser, C. (2008). Mathematical models of infectious disease transmission. *Nature Reviews Microbiology*, *6*(6), 477-487. https://doi.org/10.1038/nrmicro1845

Greenwood, B. (2013). The epidemiology of meningococcal disease in Africa. *Tropical Medicine & International Health*, *18*(12), 1568-1575. https://doi.org/10.1111/tmi.12200

Guerra, F. M., Bolotin, S., Lim, G., Heffernan, J., Deeks, S. L., Li, Y., & Crowcroft, N. S. (2017). The basic reproduction number (R_0) of measles: A systematic review. *The Lancet Infectious Diseases*, *17*(12), e420-e428. https://doi.org/10.1016/S1473-3099(17)30307-9

Hairer, E., Nørsett, S. P., and Wanner, G. (2008). *Solving ordinary differential equations I: Nonstiff problems* (2nd ed.). Springer.

Harko, T., Lobo, F. S., and Mak, M. K. (2014). Exact analytical solutions of the Susceptible-Infected-Recovered (SIR) epidemic model and of the SIR model with equal death and birth rates. *Applied Mathematics and Computation*, *236*, 184-194.

Heesterbeek, H., Anderson, R. M., Andreasen, V., Bansal, S., De Angelis, D., Dye, C., and Viboud, C. (2015). Modeling infectious disease dynamics in the complex landscape of global health. *Science*, *347*(6227).

Heffernan, J. M., Smith, R. J., and Wahl, L. M. (2005). Perspectives on the basic reproductive ratio. *Journal of the Royal Society Interface*, *2*(4), 281-293.

Hethcote, H. W. (2000). The mathematics of infectious diseases. *SIAM Review*, *42*(4), 599-653. https://doi.org/10.1137/S0036144500371907

Hilborn, R., and Mangel, M. (1997). *The ecological detective: Confronting models with data*. Princeton University Press.

Iserles, A. (2009). *A first course in the numerical analysis of differential equations* (2nd ed.). Cambridge University Press.

Jones, K. E., Patel, N. G., Levy, M. A., Storeygard, A., Balk, D., Gittleman, J. L., and Daszak, P. (2022). Global trends in emerging infectious diseases. *Nature*, *451*(7181), 990-993.

Keeling, M. J., and Rohani, P. (2008). *Modeling infectious diseases in humans and animals*. Princeton University Press.

Kerneis, S., Koivogui, L., Magassouba, N., Koulemou, K., Lewis, R., Aplogan, A., ... & Grais, R. F. (2009). Prevalence and risk factors of Lassa seropositivity in inhabitants of the forest region of Guinea: A cross-sectional study. *PLoS Neglected Tropical Diseases*, *3*(11), e548.

Kermack, W. O., and McKendrick, A. G. (1927). A contribution to the mathematical theory of epidemics. *Proceedings of the Royal Society of London Series A, 115*(772), 700-721. https://doi.org/10.1098/rspa.1927.0118

Lagos State Government. (2022). *Lagos State statistical yearbook 2022*. Lagos Bureau of Statistics.

Levin, S. A., Grenfell, B., Hastings, A., and Perelson, A. S. (1997). Mathematical and computational challenges in population biology and ecosystems science. *Science, 275*(5298), 334-343.

Levins, R. (1966). The strategy of model building in population biology. *American Scientist, 54*(4), 421-431.

Metcalf, C. J. E., Edmunds, W. J., and Lessler, J. (2015). Six challenges in modelling for public health policy. *Epidemics, 10*, 93-96.

Metcalf, C. J. E., Morris, D. H., and Park, S. W. (2017). Mathematical models for infectious disease dynamics. *Interface Focus, 7*(5), 20170018.

Molesworth, A. M., Cuevas, L. E., Connor, S. J., Morse, A. P., & Thomson, M. C. (2003). Environmental risk and meningitis epidemics in Africa. *Emerging Infectious Diseases, 9*(10), 1287-1293.

Mooney, D. D., and Swift, R. J. (1999). *A course in mathematical modeling*. Mathematical Association of America.

Morens, D. M., Folkers, G. K., and Fauci, A. S. (2020). The challenge of emerging and re-emerging infectious diseases. *Nature, 430*(6996), 242-249.

Muka K.O and Ikhile M.N.O.(2015). A Diagraph Theoretic Parallelism in Block methods. Afrika matematika, Vol 26. No 7 and 8, pp 1651-1667.

Nasir, S. G., Aliyu, G. G., Ya'u, I., Gadanya, M., Mohammad, M., Zubair, M., ... & Balogun, M. S. (2021). From Kano to Zamfara: Why do measles outbreaks persist in Northern Nigeria? *New Microbes and New Infections*, *43*, 100906. https://doi.org/10.1016/j.nmni.2021.100906

National Population Commission. (2023). *Nigeria demographic and health survey 2018*. National Population Commission and ICF.

Nigeria Centre for Disease Control. (2020). *Annual epidemiological report 2020*. NCDC Publications.

Nigeria Centre for Disease Control. (2022). *Lassa fever situation report: Epidemiological week 52, 2022*. NCDC.

Nigeria Centre for Disease Control. (2023). Weekly epidemiological report: Measles surveillance. *NCDC Weekly Report, 45*(12), 1-15. Retrieved from https://ncdc.gov.ng/reports/weekly

Nigeria Centre for Disease Control. (2024). *Annual report on Lassa fever surveillance in Nigeria*. NCDC Publications.

Okuonghae, D., and Omame, A. (2020). Analysis of a mathematical model for COVID-19 population dynamics in Lagos, Nigeria. *Chaos, Solitons & Fractals*, *139*, 110032. https://doi.org/10.1016/j.chaos.2020.110032

Omame, A., Isiguzo, E. A., Abbas, M., Abdel-Aty, A. H., and Onyenegecha, C. P. (2021). A mathematical study of a generalized SEIR model of COVID-19 transmission in Nigeria. *Alexandria Engineering Journal*, *60*(5), 4529-4545. https://doi.org/10.1016/j.aej.2021.03.041

Oreskes, N., Shrader-Frechette, K., and Belitz, K. (1994). Verification, validation, and confirmation of numerical models in the earth sciences. *Science*, *263*(5147), 641-646.

Pérez, F., and Granger, B. E. (2007). IPython: A system for interactive scientific computing. *Computing in Science & Engineering*, *9*(3), 21-29.

Peter, O. J., Qureshi, S., Yusuf, A., Al-Shomrani, M., and Idowu, A. A. (2021). A new mathematical model of COVID-19 using real data from Pakistan. *Results in Physics*, *24*, 104098. https://doi.org/10.1016/j.rinp.2021.104098

Pilkey, O. H., and Pilkey-Jarvis, L. (2007). *Useless arithmetic: Why environmental scientists can't predict the future*. Columbia University Press.

Regan, H. M., Colyvan, M., and Burgman, M. A. (2002). A taxonomy and treatment of uncertainty for ecology and conservation biology. *Ecological Applications*, *12*(2), 618-628.

Roberts, M., Andreasen, V., Lloyd, A., and Pellis, L. (2015). Nine challenges for deterministic epidemic models. *Epidemics*, *10*, 49-53.

Rothman, K. J., Greenland, S., and Lash, T. L. (2021). *Modern epidemiology* (4th ed.). Lippincott Williams and Wilkins.

Saltelli, A., Ratto, M., Andres, T., Campolongo, F., Cariboni, J., Gatelli, D., Saisana, M., & Tarantola, S. (2008). *Global sensitivity analysis: The primer*. John Wiley & Sons.

Shampine, L. F. (1994). *Numerical solution of ordinary differential equations*. Chapman & Hall.

Shittu, A. M., Olayinka, G. O., and Falaye, B. J. (2020). Mathematical modeling of the dynamics of COVID-19 in Nigeria. *Applied Mathematics*, *11*(12), 1276-1295. https://doi.org/10.4236/am.2020.1112085

Süli, E., and Mayers, D. F. (2003). *An introduction to numerical analysis*. Cambridge University Press.

Thompson, J. M. T., and Stewart, H. B. (2002). *Nonlinear dynamics and chaos* (2nd ed.). John Wiley and Sons.

Trotter, C. L., and Greenwood, B. M. (2007). Meningococcal carriage in the African meningitis belt. *The Lancet Infectious Diseases*, *7*(12), 797-803.

UNICEF Nigeria. (2022). *Nigeria multiple indicator cluster survey 2021*. UNICEF Nigeria Country Office.

van den Driessche, P. (2017). Reproduction numbers of infectious disease models. *Infectious Disease Modelling*, *2*(3), 288-303.

Vynnycky, E., and White, R. G. (2010). *An introduction to infectious disease modelling*. Oxford University Press.

Wang, X., et al. (2021). Transmission dynamics and control of Lassa fever: A mathematical modeling approach. *Infectious Disease Modelling*, *6*, 1323-1339.

World Health Organization. (2017). *Meningococcal disease outbreak response in sub-Saharan Africa: WHO guideline*. World Health Organization.

World Health Organization. (2019). Nigeria is now free of wild polio virus. *WHO Africa Regional Office*. Retrieved from https://www.afro.who.int/news/nigeria-now-free-wild-polio-virus

World Health Organization. (2023). *Infectious diseases*. https://www.who.int/health-topics/infectious-diseases

World Health Organization. (2023). *Measles fact sheet*. WHO Global Health Observatory Data Repository. Retrieved from https://www.who.int/news-room/fact-sheets/detail/measles

World Health Organization. (2023). *Measles fact sheet*. WHO Press.

World Health Organization. (2024). *Lassa fever fact sheet*. WHO Press.

World Health Statistics 2023: Monitoring Health or the SDGs).

Yaro, S., Lourd, M., Traoré, Y., Njanpop-Lafourcade, B. M., Sawadogo, A., Sangare, L., ... and Gessner, B. D. (2006). Epidemiological and molecular characteristics of a highly lethal pneumococcal meningitis epidemic in Burkina Faso. *Clinical Infectious Diseases*, *43*(6), 693-700.

APPENDIX

Appendix A: Mathematica Code for Disease A (Measles)

A.1 Heun's Method Implementation

```
(* Measles - Heun *)beta = 0.9; gamma = 0.1; Q = 1000;

S0 = 990; I0 = 10; R0 = 0;

HeunStep[f_, {t_, y_}, h_] := Module[{k1, k2},k1 = f[t, y]; k2 = f[t + h, y + h*k1];

  {t + h, y + (h/2)*(k1 + k2)}];

fMeasles[t_, {S_, I_, R_}] := {-beta*S*I/Q, beta*S*I/Q - gamma*I, gamma*I};h = 0.1; tmax =
10; steps = Floor[tmax/h];

heunSol = NestList[HeunStep[fMeasles, #, h] &, {0, {S0, I0, R0}}, steps];

ListLinePlot[heunSol[[All, 2, 1]], DataRange -> {0, tmax},PlotLabel -> "Measles (Heun) -
Susceptible", AxesLabel -> {"t", "S(t)"}]

ListLinePlot[heunSol[[All, 2, 2]], DataRange -> {0, tmax},PlotLabel -> "Measles (Heun) -
Infected", AxesLabel -> {"t", "I(t)"}]

ListLinePlot[heunSol[[All, 2, 3]], DataRange -> {0, tmax},PlotLabel -> "Measles (Heun) -
Recovered", AxesLabel -> {"t", "R(t)"}]
```

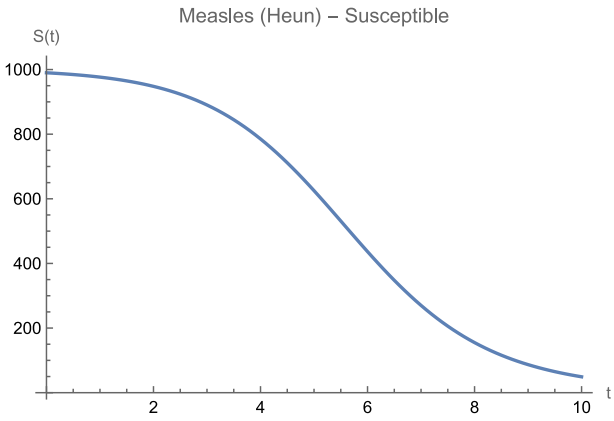

Figure 1: Measles S -Heun Method

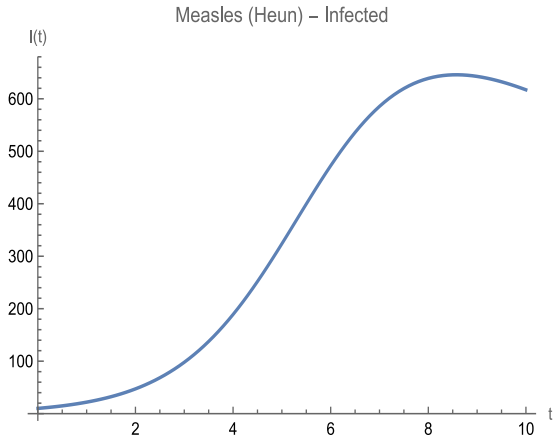

Figure 2: Measles I- Heun Method

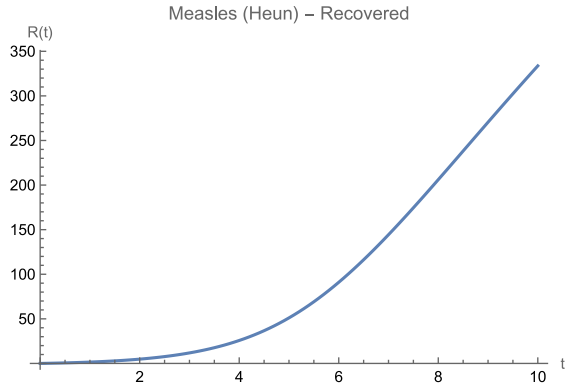

Figure 3: Measles R - Heun Method

A.2 Midpoint Method Implementation

(* Measles - Midpoint *)

```
MidpointStep[f_, {t_, y_}, h_] := Module[{k1, k2},k1 = f[t, y]; k2 = f[t + h/2, y + (h/2)*k1];
  {t + h, y + h*k2}];
midSol = NestList[MidpointStep[fMeasles, #, h] &, {0, {S0, I0, R0}}, steps];
ListLinePlot[midSol[[All, 2, 1]], DataRange -> {0, tmax},PlotLabel -> "Measles (Midpoint) -
Susceptible", AxesLabel -> {"t", "S(t)"}]
ListLinePlot[midSol[[All, 2, 2]], DataRange -> {0, tmax},PlotLabel -> "Measles (Midpoint) -
Infected", AxesLabel -> {"t", "I(t)"}]
ListLinePlot[midSol[[All, 2, 3]], DataRange -> {0, tmax},PlotLabel -> "Measles (Midpoint) -
Recovered", AxesLabel -> {"t", "R(t)"}]
```

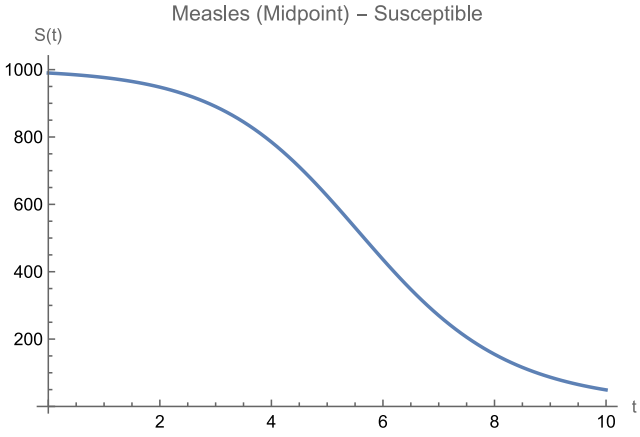

Figure 4: Measles S - Midpoint Method

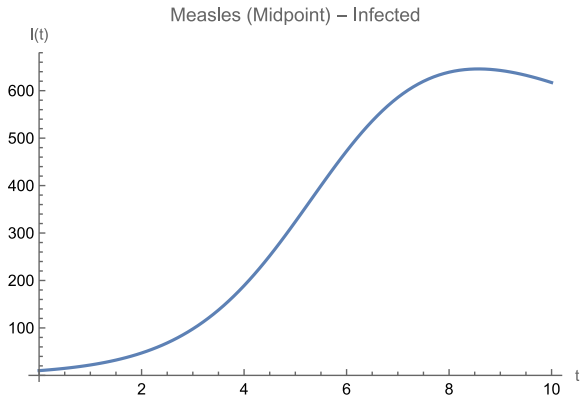

Figure 5: Measles I - Midpoint Method

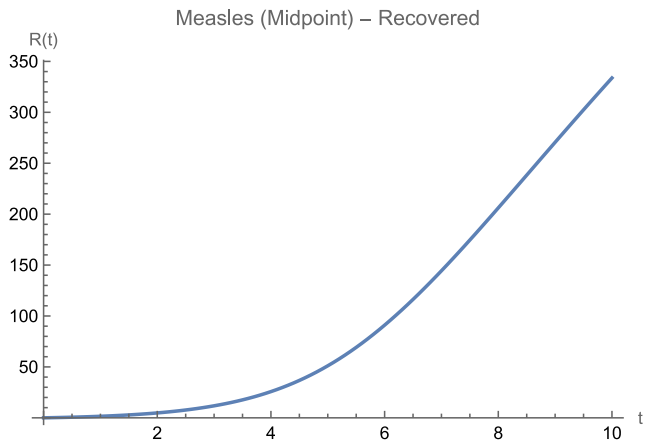

Figure 6: Measles R - Midpoint Method

A.3 Ralston's Method Implementation

```
(* Measles - Ralston *)

RalstonStep[f_, {t_, y_}, h_] := Module[{k1, k2}, k1 = f[t, y]; k2 = f[t + (2*h)/3, y +
(2*h/3)*k1];

  {t + h, y + (h/4)*(k1 + 3*k2)}];

ralSol = NestList[RalstonStep[fMeasles, #, h] &, {0, {S0, I0, R0}}, steps];

ListLinePlot[ralSol[[All, 2, 1]], DataRange -> {0, tmax},PlotLabel -> "Measles (Ralston) -
Susceptible", AxesLabel -> {"t", "S(t)"}]

ListLinePlot[ralSol[[All, 2, 2]], DataRange -> {0, tmax},PlotLabel -> "Measles (Ralston) -
Infected", AxesLabel -> {"t", "I(t)"}]

ListLinePlot[ralSol[[All, 2, 3]], DataRange -> {0, tmax},PlotLabel -> "Measles (Ralston) -
Recovered", AxesLabel -> {"t", "R(t)"}]
```

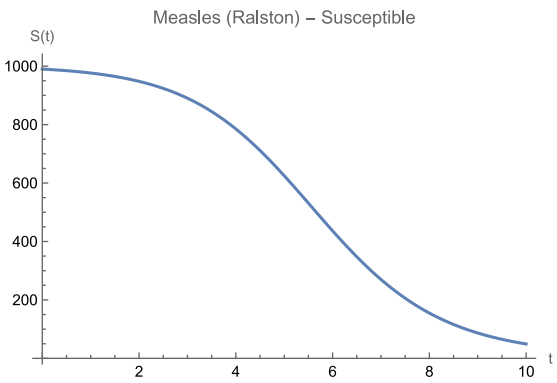

Figure 7: Measles S - Ralston Method

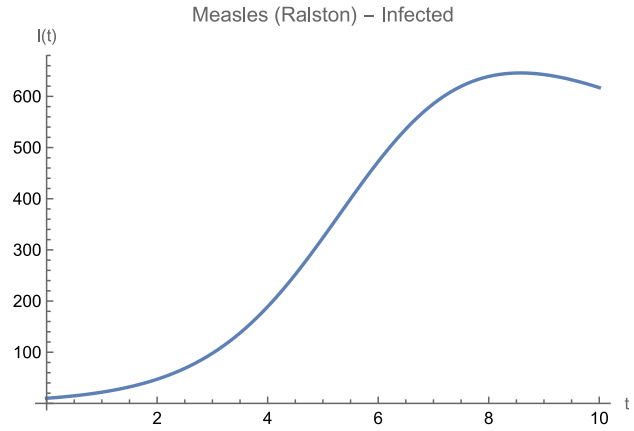

Figure 8: Measles I - Ralston Method

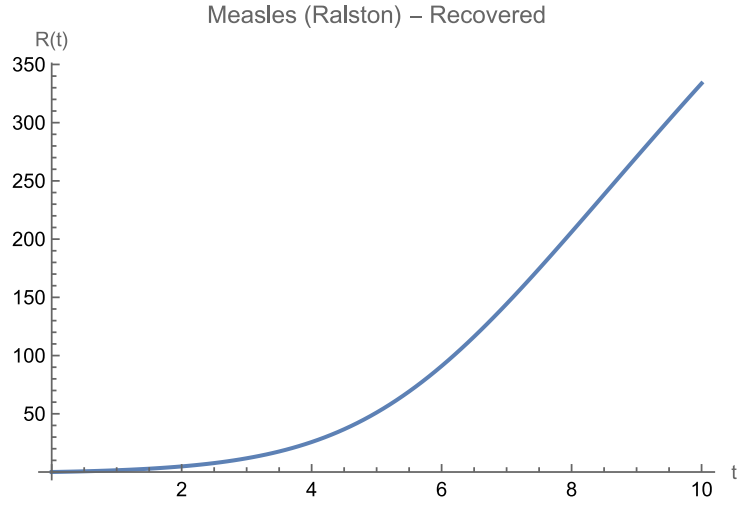

Figure 9: Measles R - Ralston Method

Appendix B: Mathematica Code for Disease B (Influenza)

B.1 Heun's Method Implementation

(* Influenza - Heun *)beta = 0.3; gamma = 0.1; omega = 0.05; Q = 1000;

S0 = 900; I0 = 100; R0 = 0;

```
HeunStep[f_, {t_, y_}, h_] := Module[{k1, k2},
  k1 = f[t, y]; k2 = f[t + h, y + h*k1];
  {t + h, y + (h/2)*(k1 + k2)}];
fInfluenza[t_, {S_, I_, R_}] := {-beta*S*I/Q + omega*R, beta*S*I/Q - gamma*I, gamma*I - omega*R};
h = 0.1; tmax = 10; steps = Floor[tmax/h];
heunInf = NestList[HeunStep[fInfluenza, #, h] &, {0, {S0, I0, R0}}, steps];
ListLinePlot[heunInf[[All, 2, 1]], DataRange -> {0, tmax},PlotLabel -> "Influenza (Heun) - Susceptible", AxesLabel -> {"t", "S(t)"}]
ListLinePlot[heunInf[[All, 2, 2]], DataRange -> {0, tmax},PlotLabel -> "Influenza (Heun) - Infected", AxesLabel -> {"t", "I(t)"}]
ListLinePlot[heunInf[[All, 2, 3]], DataRange -> {0, tmax},PlotLabel -> "Influenza (Heun) - Recovered", AxesLabel -> {"t", "R(t)"}]
```

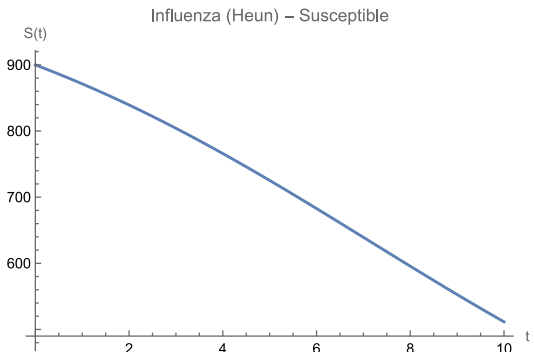

Figure 10: Influenza S – Heun Method

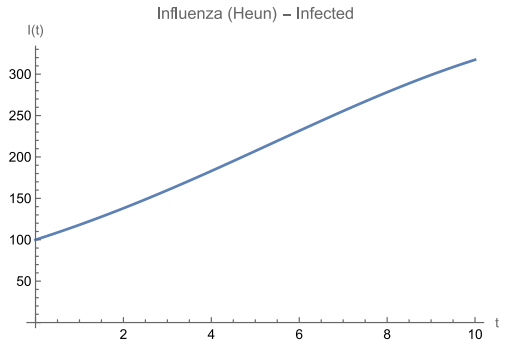

Figure 11: Influenza I – Heun Method

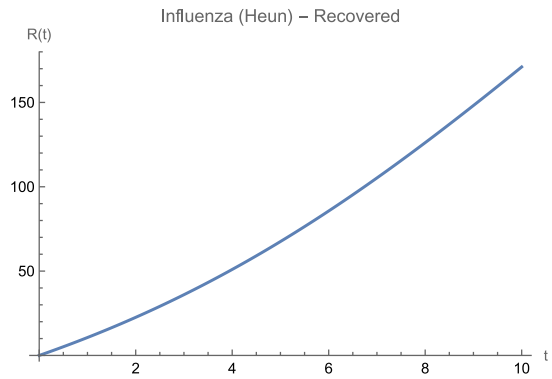

Figure 12: Influenza R – Heun Method

B.2 Midpoint Method Implementation

```
(* Influenza - Midpoint *)

MidpointStep[f_, {t_, y_}, h_] := Module[{k1, k2},k1 = f[t, y]; k2 = f[t + h/2, y + (h/2)*k1];

  {t + h, y + h*k2}];

midInf = NestList[MidpointStep[fInfluenza, #, h] &, {0, {S0, I0, R0}}, steps];

ListLinePlot[midInf[[All, 2, 1]], DataRange -> {0, tmax},

 PlotLabel -> "Influenza (Midpoint) - Susceptible", AxesLabel -> {"t",

"S(t)"}]ListLinePlot[midInf[[All, 2, 2]], DataRange -> {0, tmax},

 PlotLabel -> "Influenza (Midpoint) - Infected", AxesLabel -> {"t",

"I(t)"}]ListLinePlot[midInf[[All, 2, 3]], DataRange -> {0, tmax},

PlotLabel -> "Influenza (Midpoint) - Recovered", AxesLabel -> {"t", "R(t)"}]
```

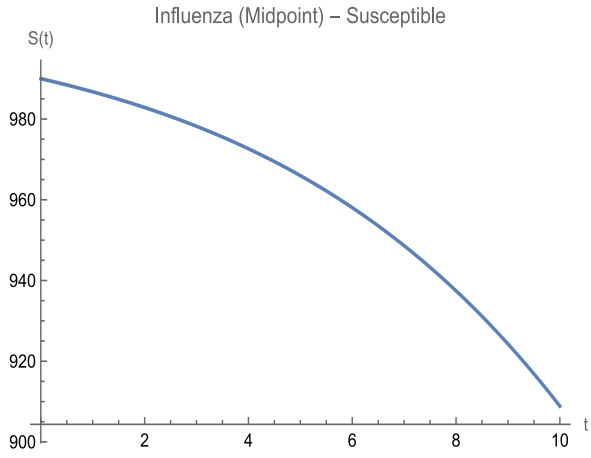

Figure 13: Influenza S – Midpoint Method

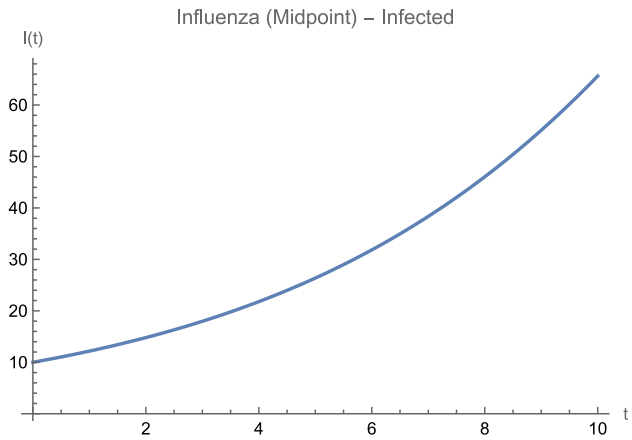

Figure 14: Influenza I – Midpoint Method

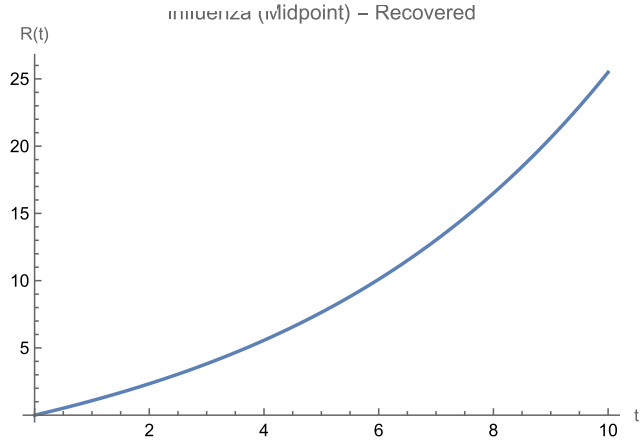

Figure 15: Influenza R – Midpoint Method

B.3 Ralston's Method Implementation

```
(* Influenza - Ralston *)RalstonStep[f_, {t_, y_}, h_] := Module[{k1, k2},k1 = f[t, y]; k2 = f[t +
(2*h)/3, y + (2*h/3)*k1];
  {t + h, y + (h/4)*(k1 + 3*k2)}];
ralInf = NestList[RalstonStep[fInfluenza, #, h] &, {0, {S0, I0, R0}}, steps];
ListLinePlot[ralInf[[All, 2, 1]], DataRange -> {0, tmax},PlotLabel -> "Influenza (Ralston) -
Susceptible", AxesLabel -> {"t", "S(t)"}]
```

```
ListLinePlot[ralInf[[All, 2, 2]], DataRange -> {0, tmax},PlotLabel -> "Influenza (Ralston) -
Infected", AxesLabel -> {"t", "I(t)"}]

ListLinePlot[ralInf[[All, 2, 3]], DataRange -> {0, tmax},PlotLabel -> "Influenza (Ralston) -
Recovered", AxesLabel -> {"t", "R(t)"}]
```

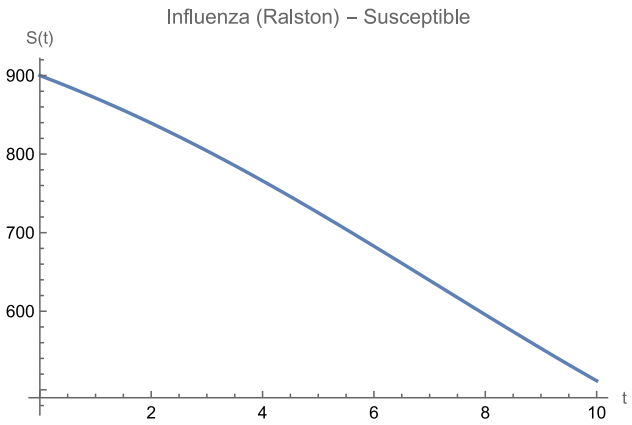

Figure 16: Influenza S – Ralston Method

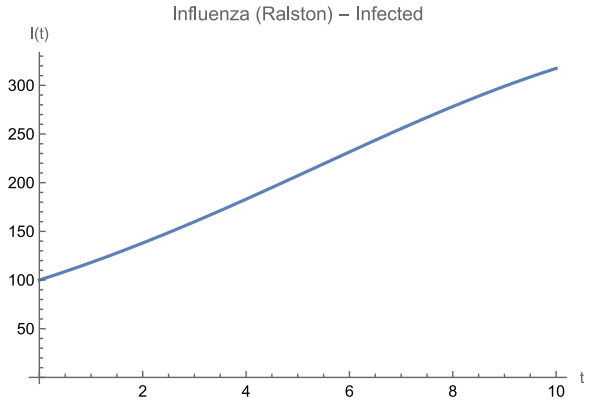

Figure 17: Influenza I – Ralston Method

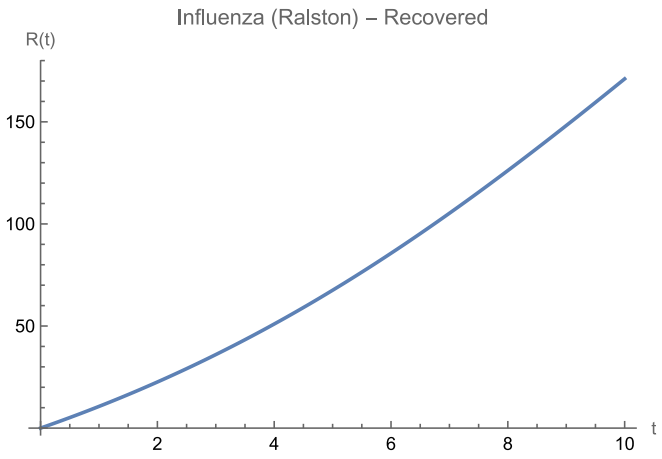

Figure 18: Influenza R – Ralston Method

Appendix C: Mathematica Code for Disease C (Lassa Fever)

C.1 Heun's Method Implementation

```
(* Lassa - Heun *)beta1 = 0.25; beta2 = 0.01; gamma = 0.1; delta = 0.05; mu = 0.01; Q = 1000;

S0 = 990; I0 = 10; R0 = 0; D0 = 0;

HeunStep[f_, {t_, y_}, h_] := Module[{k1, k2},k1 = f[t, y]; k2 = f[t + h, y + h*k1];

  {t + h, y + (h/2)*(k1 + k2)}];

fLassa[t_, {S_, I_, R_, D_}] := {-beta1*S*I/Q - beta2*S + mu*Q - mu*S,beta1*S*I/Q + beta2*S
- (gamma + delta + mu)*I,gamma*I - mu*R,delta*I};

h = 0.1; tmax = 10; steps = Floor[tmax/h];

heunLas = NestList[HeunStep[fLassa, #, h] &, {0, {S0, I0, R0, D0}}, steps];

ListLinePlot[heunLas[[All, 2, 1]], DataRange -> {0, tmax},PlotLabel -> "Lassa (Heun) -
Susceptible", AxesLabel -> {"t", "S(t)"}]

ListLinePlot[heunLas[[All, 2, 2]], DataRange -> {0, tmax},PlotLabel -> "Lassa (Heun) -
Infected", AxesLabel -> {"t", "I(t)"}]

ListLinePlot[heunLas[[All, 2, 3]], DataRange -> {0, tmax},PlotLabel -> "Lassa (Heun) -
Recovered", AxesLabel -> {"t", "R(t)"}]

ListLinePlot[heunLas[[All, 2, 4]], DataRange -> {0, tmax},PlotLabel -> "Lassa (Heun) -
Deaths", AxesLabel -> {"t", "D(t)"}]
```

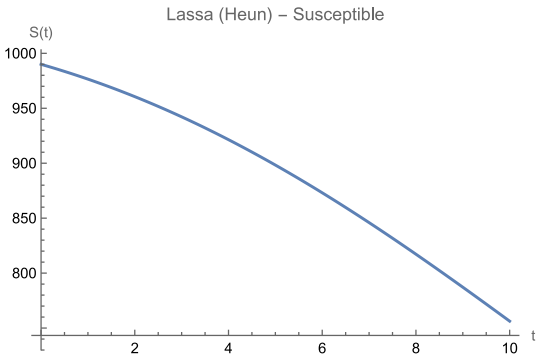

Figure 19: Lassa Fever S – Heun Method

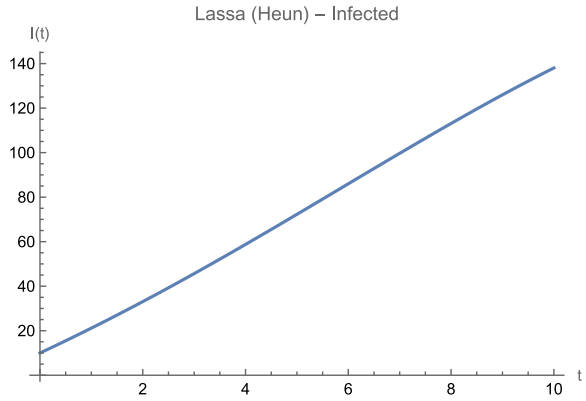

Figure 20: Lassa Fever I – Heun Method

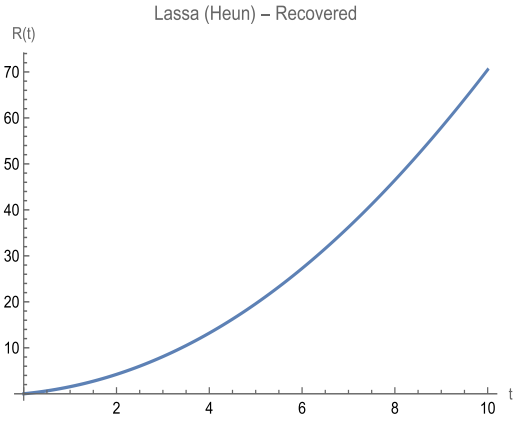

Figure 21: Lassa Fever R – Heun Method

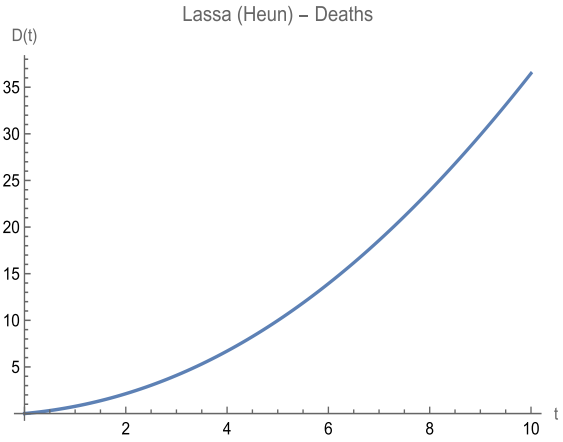

Figure 22: Lassa Fever D – Heun Method

C.2 Midpoint Method Implementation

```
(* Lassa - Midpoint *)MidpointStep[f_, {t_, y_}, h_] := Module[{k1, k2},k1 = f[t, y]; k2 = f[t +
h/2, y + (h/2)*k1];

{t + h, y + h*k2}];

midLas = NestList[MidpointStep[fLassa, #, h] &, {0, {S0, I0, R0, D0}}, steps];
```

```
ListLinePlot[midLas[[All, 2, 1]], DataRange -> {0, tmax},PlotLabel -> "Lassa (Midpoint) -
Susceptible", AxesLabel -> {"t", "S(t)"}]

ListLinePlot[midLas[[All, 2, 2]], DataRange -> {0, tmax},PlotLabel -> "Lassa (Midpoint) -
Infected", AxesLabel -> {"t", "I(t)"}]

ListLinePlot[midLas[[All, 2, 3]], DataRange -> {0, tmax},PlotLabel -> "Lassa (Midpoint) -
Recovered", AxesLabel -> {"t", "R(t)"}]

ListLinePlot[midLas[[All, 2, 4]], DataRange -> {0, tmax},PlotLabel -> "Lassa (Midpoint) -
Deaths", AxesLabel -> {"t", "D(t)"}]
```

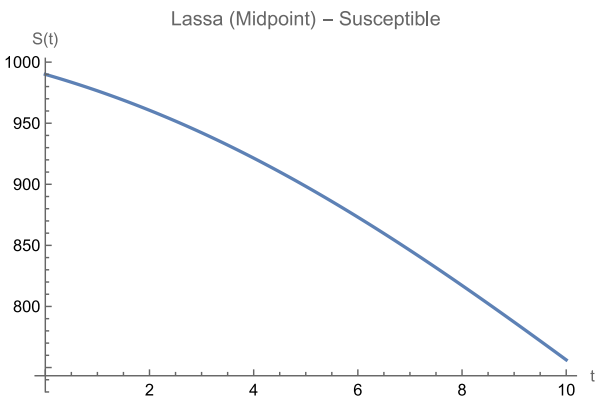

Figure 23: Lassa Fever S – Midpoint Method

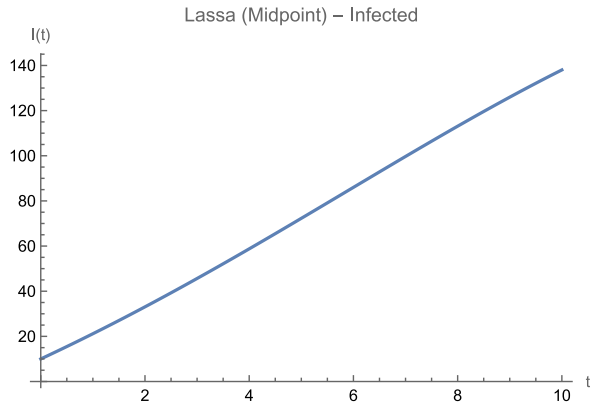

Figure 24: Lassa Fever I – Midpoint Method

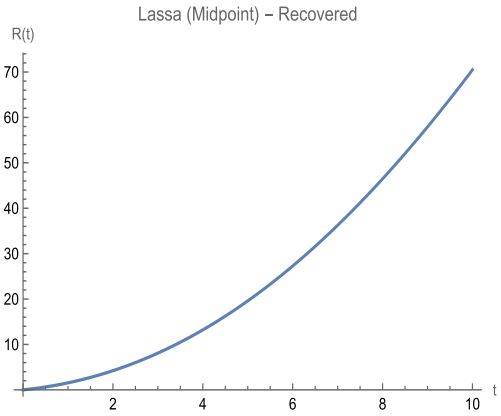

Figure 25: Lassa Fever R – Midpoint Method

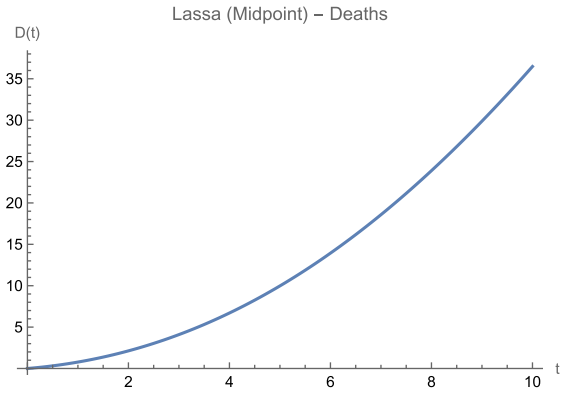

Figure 26: Lassa Fever D – Midpoint Method

C.3 Ralston's Method Implementation

```
(* Lassa - Ralston *)RalstonStep[f_, {t_, y_}, h_] := Module[{k1, k2},k1 = f[t, y]; k2 = f[t +
(2*h)/3, y + (2*h/3)*k1];

{t + h, y + (h/4)*(k1 + 3*k2)}];

ralLas = NestList[RalstonStep[fLassa, #, h] &, {0, {S0, I0, R0, D0}}, steps];

ListLinePlot[ralLas[[All, 2, 1]], DataRange -> {0, tmax},PlotLabel -> "Lassa (Ralston) -
Susceptible", AxesLabel -> {"t", "S(t)"}]

ListLinePlot[ralLas[[All, 2, 2]], DataRange -> {0, tmax},PlotLabel -> "Lassa (Ralston) -
Infected", AxesLabel -> {"t", "I(t)"}]

ListLinePlot[ralLas[[All, 2, 3]], DataRange -> {0, tmax},PlotLabel -> "Lassa (Ralston) -
Recovered", AxesLabel -> {"t", "R(t)"}]
```

ListLinePlot[ralLas[[All, 2, 4]], DataRange -> {0, tmax},PlotLabel -> "Lassa (Ralston) - Deaths", AxesLabel -> {"t", "D(t)"}]

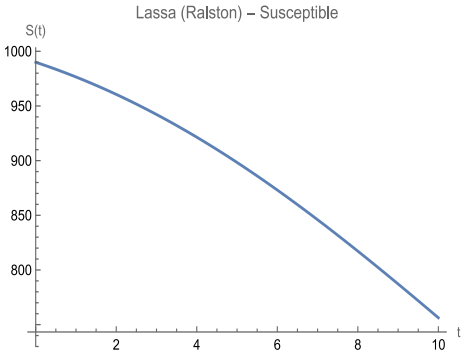

Figure 27: Lassa Fever S – Ralston Method

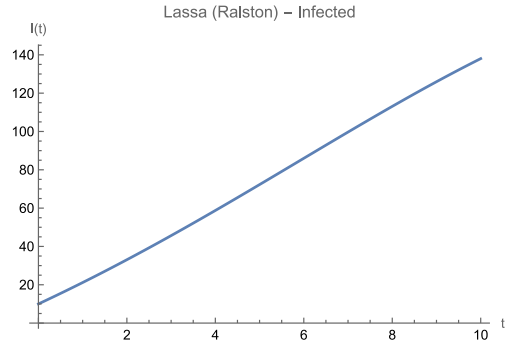

Figure 28: Lassa Fever I – Ralston Method

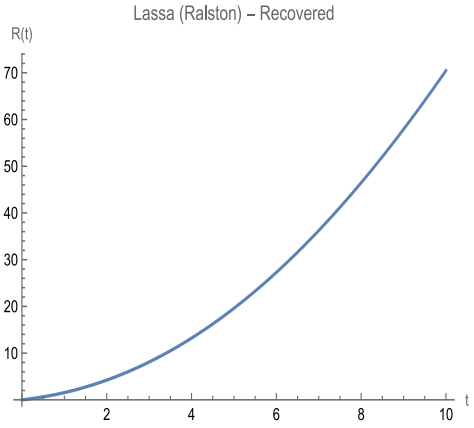

Figure 29: Lassa Fever R – Ralston Method

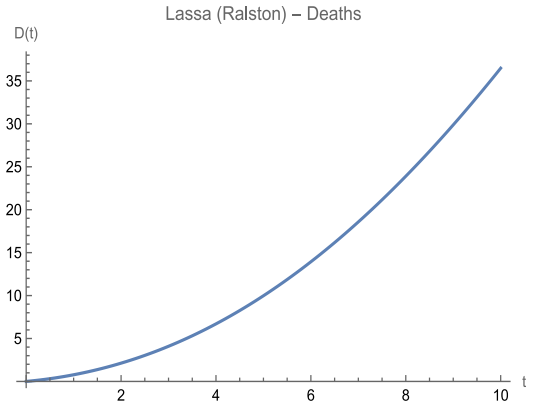

Figure 30: Lassa Fever D – Ralston Method